UPPSALA
UNIVERSITET

Digital Comprehensive Summaries of Uppsala Dissertations from the Faculty of Science and Technology 1939

Electromagnetic and Spin Properties of Hyperons

ELISABETTA PEROTTI

ACTA
UNIVERSITATIS
UPSALIENSIS
UPPSALA
2020

ISSN 1651-6214
ISBN 978-91-513-0956-9
urn:nbn:se:uu:diva-406648

Dissertation presented at Uppsala University to be publicly examined in Häggsalen, Ångströmlaboratoriet, Lägerhyddsvägen 1, Uppsala, Friday, 12 June 2020 at 13:00 for the degree of Doctor of Philosophy. The examination will be conducted in English. Faculty examiner: Dr. Luis Alvarez Ruso (Department of Theoretical Physics, Facultad de Ciencias Físicas, Universidad de Valencia).

Abstract
Perotti, E. 2020. Electromagnetic and Spin Properties of Hyperons. *Digital Comprehensive Summaries of Uppsala Dissertations from the Faculty of Science and Technology* 1939. 69 pp. Uppsala: Acta Universitatis Upsaliensis. ISBN 978-91-513-0956-9.

The study of hyperons improves our understanding of nature in multiple ways. The intrinsic properties of hadrons are not fully understood at a fundamental level. Hence, the electromagnetic properties of hyperons provide complementary information to that of the nucleon and therefore allow for a broader investigation of the structure of matter. Electromagnetic form factors have been extensively studied for the nucleon, and are now addressed also in the hyperon sector. In this thesis, the electromagnetic Σ-Λ hyperon transition form factors have been determined at low energies, in a pioneering framework that makes use of dispersion relations to combine theoretical and experimental input. Subsequently this analysis has been extended to the decuplet spin-3/2 Σ^* -Λ transition. Assuming that these transition form factors are saturated by a two-pion inelasticity, their imaginary part can be written in terms of the pion vector form factor and a pion-hyperon scattering amplitude. Chiral perturbation theory at next-to-leading order has been used to calculate the latter, while the pion vector form factor and the related pion phase-shift are known from measurements.

The spin properties of hyperons can be resolved through their weak decays. The angular distribution of their decay products displays both polarization parameters and decay asymmetry parameters. These originate from processes characterized by an interplay of partial waves and are useful for different purposes. The polarization is sensitive to the production mechanism; in the $\bar{p}p$ case, it can be used to probe the strong interaction in the non-perturbative regime while in the e^+e^- case it contains the relative phase between complex electromagnetic form factors. Decay asymmetry parameters, on the other hand, are used to construct observables that test CP violation. Additional sources of CP violation must be found to solve the problem of the baryon asymmetry in our universe. This work provides a systematic method to retrieve both polarization and decay asymmetry parameters directly from the angular distribution of the hyperon decay products.

Keywords: Electromagnetic form factors, hyperon physics, dispersion relations, QCD, chiral perturbation theory, CP violation

Elisabetta Perotti, Department of Physics and Astronomy, Nuclear Physics, Box 516, Uppsala University, SE-751 20 Uppsala, Sweden.

ISSN 1651-6214
ISBN 978-91-513-0956-9
urn:nbn:se:uu:diva-406648 (http://urn.kb.se/resolve?urn=urn:nbn:se:uu:diva-406648)

To my parents,
Daniela and Graziano

List of papers

This thesis is based on the following papers, which are referred to in the text by their Roman numerals.

I C. Granados, S. Leupold, E. Perotti.
The electromagnetic Sigma-to-Lambda hyperon transition form factors at low energies.
Eur. Phys. J., A53:117, 2017.

II E. Perotti.
Extraction of Polarization Parameters in the $\bar{p}p \to \bar{\Omega}\Omega$ Reaction.
J. Phys. Conf. Ser., 1024:012019, 2018.

III S. S. Nair, E. Perotti, S. Leupold.
Constraining P and CP violation in the main decay of the neutral Sigma hyperon.
Phys. Lett., B788:535, 2019.

IV E. Perotti, G. Fäldt, A. Kupsc, S. Leupold, J. J. Song.
Polarization observables in e^+e^- annihilation to a baryon-antibaryon pair.
Phys. Rev., D99:056008, 2019.

V O. Junker, S. Leupold, E. Perotti, T. Vitos.
Electromagnetic form factors of the transition from the spin-3/2 Σ to the Λ hyperon.
Phys. Rev., C101:015206, 2020.

Contents

1. Introduction

Give me the beat!

Norma Miller, the Queen of Swing

This thesis belongs to the branch of particle and nuclear physics, more precisely theoretical hadron physics. Hadrons are composite objects made out of *quarks*, which appear to be elementary at the energy scales currently accessible by experiments. The neutrons and the protons, constituting most of our mass, are the most well-known members of the large hadron family.

In the last decade, the field of particle physics has been largely dominated by research at high energies, both in theory and experiment. At *e.g.* the Large Hadron Collider (LHC), highly energetic protons collide, giving rise to a plethora of particles. In virtue of the famous equation $E = mc^2$, the larger the energy available, the heavier the newly produced particles can be. These particles are the same as those that were produced just after the Big Bang, and that decayed shortly after. Even if they do not interfere with our daily life, their discovery is a crucial step towards the understanding of our existence. Looking for specific patterns when categorizing their properties reveals that nature obeys quite precise rules. Theoretical physicists try to figure out which symmetries and conservation laws govern the production and decay of particles in order to describe the experimental findings and especially to make further predictions. Theories provide guidance when deciding what to search for in experiments. The most successful theory, the Standard Model (SM) of particle physics, will be briefly introduced later in this chapter.

The SM describes a wide range of phenomena accurately and precisely, but it is not the final theory of our universe. Four often mentioned shortcomings are: i) it does not explain dark matter and dark energy, ii) it does not include neutrino masses, iii) it does not predict the observed amount of matter-antimatter asymmetry and iv) it does not incorporate gravity. These topics are currently under investigation together with possible beyond-SM extensions. For now, they still constitute open questions. The scientific community has basically two complementary ways of seeking new physics answers: colliding particles at higher and higher energies in order to (hopefully!) discover heavier particles or producing a vast amount of already known particles and study them in greater detail. Even the latter option can indicate new, hidden physics. In this spirit, we are now approaching the era of high-precision measurements.

The general philosophy here is to study further the properties of already discovered particles, in particular those that can be calculated and measured with high precision. This because even tiny discrepancies between experimentally and theoretically obtained observables hint at physics beyond the SM. This approach is very suitable for research at lower energies, to which my thesis belongs. Specifically, part of my research relates to the baryon asymmetry problem. Hyperon weak decays can be exploited to look for processes where the violation of the combined charge conjugation and parity (CP) symmetry could occur.

A second and major aspect of my thesis is to improve the understanding of the structure of matter. The focus has not been directly on nucleons but on hyperons, a choice that can seem "strange" at first. So far, the available information on the hyperon electromagnetic and spin properties is limited, but it is increasing due to the rising interest from the hadron physics community. The structural similarities and differences between nucleons and hyperons make the latter strategical candidates to be investigated further. Concretely, the future goal will be to compare the hyperon and nucleon electromagnetic form factors and the corresponding low-energy quantities (electric charge, magnetic moment, electric and magnetic radii), in order to gain insight into the behavior of the quarks confined within these hadrons.

1.1 Thesis outline

I have assumed that the reader is somewhat familiar with the subject of this thesis, hadron physics, and has a basic knowledge of modern theory tools in particle physics like quantum field theory and effective field theory. I have selected some relevant material and organized it as follows: Chapter 1 skims through the foundation of elementary particle physics, *i.e.* the SM, with emphasis on the symmetries of the strong sector. The concept of form factors is also introduced. They allow for a general characterization of composite objects, even when the intrinsic structure of said objects is not yet fully understood. This introductory chapter ends with a brief summary of the scientific questions addressed in my work. In chapters 2 and 3, the theoretical tools used throughout my research are presented: effective field theory and dispersion theory. These chapters are more technical since they lay the foundation for the main achievement of this thesis, the determination of the low-energy transition form factors of hyperons. In particular, I have tried to clarify which complications arise when the low-lying baryons are included in the chiral effective theory and how this is achieved. The necessity to incorporate the vector mesons via dispersion relations is also motivated. Changing topic, chapter 4 discusses the advantages of the weak parity violating decays of hyperons. Systematic methods for the extraction of polarization parameters and decay asymmetry parameters are presented. This is the result of a fruitful collab-

oration with the Uppsala experimental hadron group. Lastly, a popularized summary in Swedish is given in chapter 5.

1.2 From elementary to composite

The SM Lagrangian aims to describe the physics of our world from first principles. Only elementary particles enter its formalism. However, when studying composite objects like hadrons and atoms, the SM is not directly useful. One of the reasons why is that at different energy scales, different degrees of freedom (DOF) become relevant. Therefore, other tools are needed, which will be encountered later in this thesis. The role of the SM, in this case, is to provide a microscopic foundation for these other, more effective tools.

The elementary matter particles in the SM are grouped into two classes of fermions – leptons and quarks – that both come in three generations. The leptons are the electron, the muon and the tau, accompanied by the respective neutrino. The charged leptons interact through the electromagnetic and weak force, whereas the neutral ones interact only through the latter. For each lepton, a corresponding antilepton exists[1]. The quarks, often referred to as building blocks, are named after their *flavor*: up, down, charm, strange, top and bottom. They carry electric, color and weak charge, which means that they interact via the electromagnetic, strong and weak force. For each quark, a corresponding antiquark with opposite charges exists.

The visible matter in our universe (not more than 5% of its total mass) is made of baryonic matter [1]. Baryons are hadrons composed of three quarks, while mesons are hadrons composed of a quark-antiquark pair. For example, two up quarks and a down quark form (in a naïve picture) a proton, while an up quark together with a down antiquark form a positively charged pion. The hyperons are the main characters of this thesis, *i.e.* baryons containing strange quarks. In addition to meson and baryons, combinations of quarks, antiquarks and gluons seem to exist, though their existence is difficult to unambiguously prove.

An atomic nucleus is composed of nucleons, *i.e.* protons and neutrons, bound together by the strong nuclear force. The nucleus is positively charged. An atom consists of a nucleus electromagnetically bound to a cloud of negatively charged electrons, resulting in a neutral object. Most of the atomic mass comes from the nucleus.

[1] Actually, neutrinos might be Majorana particles, *i.e.* indistinguishable from their own antiparticle. This scenario is often considered to address beyond-SM physics.

1.3 The origin of quarks

By the beginning of the 1960s, a multitude of hadrons in addition to the nucleons had been discovered. They could not all be elementary! In particular, some of these new particles were called "strange" in the sense that their behavior could not be understood at first: Even if they could be produced in strongly interacting processes, they did not seem to decay strongly, based on the relatively long distance they were able to travel before decaying. The new particles could be categorized according to their quantum numbers, indicating that some deeper symmetry and therefore conservation laws were hiding behind the observed patterns. These strange behaviors could be explained by introducing a new quantum number, called *strangeness*, which must be conserved by the strong interaction (preventing strong decays) but broken by the weak interaction (allowing weak decays). The discovery of particles carrying strangeness was crucial to reveal that they could be classified according to the underlying flavor $SU(3)$ symmetry, also known as the Eightfold Way [2–4]. Based on this organizational scheme, the existence of a triple-strange baryon, the Ω^-, was predicted a few years prior discovery, confirming the success of the Eightfold Way [5]. Shortly after, this led to the development of the concept of quark. Assuming to be built out of quarks of different flavors, the hadrons could be organized in the quark model, independently accomplished by Gell-Mann [6] and Zweig [7] in 1964.

Note that this model requires that the quarks must carry non-integer multiples of the electric charge ($2/3$ and $-1/3$) in order to add up to integer numbers for the hadrons they form. This feature was strongly criticized at the beginning, to the point that quarks were believed to be only mathematical entities. It became more accepted when it was understood that the nature of the quarks prevents them from being observed directly. The hadrons, which can be detected in experiments, namely need be *colorless*. The concept of color [8] was introduced as a new unobservable quantum number in order to justify the existence of the spin-3/2 state Δ^{++} [9]. According to the quark model, this baryon consists of three up quarks, each with "spin up". This results in a completely symmetric wavefunction under the exchange of two quarks, at odds with the spin-statistics theorem. Color solves the problem by antisymmetrizing the wavefunction, obtaining $\varepsilon^{abc} u_{a\uparrow}(x) u_{b\uparrow}(x) u_{c\uparrow}(x)$.

In the late 1960s, the composite nature of the nucleon was finally confirmed by inelastic electron-proton scattering experiments [10]. The existence of quarks had been proven! At the same time, the puzzling finding of an anomalously large proton magnetic moment [11] had also been explained. Since the 1930s, the disagreement between the experimental value and Dirac's prediction, obtained under the hypothesis of a point-like proton, had raised many questions.

1.4 The Standard Model

The SM of particle physics [12–15] builds on a few crucial ingredients: the matter particles (quarks, leptons) interacting through three fundamental forces[2] (electromagnetic, weak, strong), each represented by the respective mediators (photon, Z and $W^{\pm}$ bosons, gluons). Last but not least, the Higgs boson, which really makes the SM not just an abstract model, but an actual description of nature.

The electromagnetic force is characterized by its infinite range of interaction and is therefore mediated by a massless neutral particle, the photon. The weak force is mediated by massive bosons and hence, it is suppressed at low energies; the Z boson is electrically neutral and interacts with particles of the same type, while the $W^{\pm}$ boson changes lepton or quark flavor. These three gauge bosons self-interact, having non-zero weak isospin charge. The strong force is mediated by gluons, which also self-interact since they carry a color charge. The quarks are confined inside a hadron by the strong force. It is worth stressing that although hadrons do not enter the SM Lagrangian themselves, the quark model is incorporated in the SM in the sense that it can be explained by the symmetries and conserved charges of the underlying theory of the strong interaction. This theory is known as quantum chromodynamics (QCD), and constitutes the SM together with the unified electroweak theory of Glashow, Weinberg and Salam. The theory of electromagnetic interactions, quantum electrodynamics (QED), emerges from the latter.

1.4.1 Gauge symmetries and masses

The SM is a quantum field theory, meaning that particles are described by excitation of fields around a ground state. In particular, it is a gauge theory with symmetry group

$$SU(3)_C \times SU(2)_L \times U(1)_Y .$$

The underlying gauge group of QCD is color $SU(3)_C$, while the electroweak sector is described by the $SU(2)_L \times U(1)_Y$ chiral gauge group. Why the SM builds on the requirement of gauge invariance is explained in most quantum field theory books, *e.g.* [14,16]. The guiding principle to follow when building a gauge theory is to demand invariance of the full theory under a specific set of local, *i.e.* spacetime dependent, transformations. The hard task is indeed to find the appropriate symmetries to be chosen as local, based on the observation of our world. The rest, *i.e.* the dynamics, will follow automatically. This is one of the enormous advantages of renormalizable gauge theories: there is no need to find all allowed interaction terms one by one. This is because

[2]The gravitational force is not taken into account in the SM. It can be neglected since it is much weaker than the other forces at the energies reached by particle accelerators.

they naturally appear as a consequence of imposing the symmetry. Gauge symmetries demand interactions and dictate their form.

An essential step to achieve gauge invariance is to introduce spin-1 fields, which have to transform in such a way that the additional terms arising from the various gauge transformations cancel each other. These vector fields can be interpreted as mediators of the three fundamental forces. To begin with, they need to be massless; explicit mass terms would spoil the gauge invariance and therefore cannot be added to the Lagrangian in a straightforward way. However, it has been experimentally found that some of them, namely the $W^{\pm}$ and Z bosons, are massive. Spontaneous symmetry breaking (SSB), more specifically the Higgs mechanism, provides an elegant solution to this problem [17, 18]. Even quarks and charged leptons acquire their mass by interacting with the Higgs scalar field via Yukawa-type interactions. In this way, massive gauge bosons and massive chiral fermions are obtained, without abandoning the requirement of gauge invariance. On the other hand, massless particles (photon, neutrinos, gluons) do not couple to the Higgs field. Neutrinos are considered massless in the SM, but they do indeed have small, non-zero masses. This property is required to explain the phenomenon of neutrino oscillations [19–21].

The key point of the SSB consists in the fact that the gauge symmetry is broken by the non-zero vacuum expectation value developed by the Higgs field. In simpler words, the minima of the Higgs potential, *i.e.* configurations of lowest energy, are not symmetric with respect to the full symmetry group of the Lagrangian. The mass terms develop naturally when the Higgs field is expanded around any of these ground states, in terms of massless scalar fields (Goldstone bosons [22]) and a massive one (Higgs boson)[3]. Note that the expression SSB can be misleading; once the Lagrangian has been rewritten in terms of these new fields, the full symmetry of the Lagrangian is not lost, as it might seem, but just "hidden" in the field redefinition. In the SM, it is the $SU(2)_L \times U(1)_Y$ symmetry to be broken down to $U(1)_Q$, giving rise to three Goldstone bosons. They can be removed from the theory, turning into additional DOF for the now massive $W^{\pm}$ and Z bosons. This operation can be performed since the spontaneously broken symmetry is local. The SM Lagrangian possesses also global symmetries on top of the local ones. Some of these are exact symmetries, others are just approximate *i.e.* realized only in a certain limit.

[3]The SM implements the Higgs mechanism in the simplest way and predicts the existence of only one Higgs boson. Possible extensions of the SM include more generations of Higgs fields [23].

1.4.2 QCD and the strong interaction

Even if the similarities between the electroweak theory and QCD are many, I will now focus on the strong interaction and its implications. It is instructive to consider the QCD Lagrangian in its compact form:

$$\mathscr{L}_{\text{QCD}} = -\frac{1}{2}\text{tr}\,(G_{\mu\nu}G^{\mu\nu}) + \bar{q}(i\not{D} - \mathscr{M})q. \tag{1.1}$$

For completeness, it is also expressed in explicit form, where summation over repeated indices (color c, flavor f, spinor s) is understood,

$$\begin{aligned}\mathscr{L}_{\text{QCD}} = &-\frac{1}{4}\left((\partial_\mu A^a_\nu - \partial_\nu A^a_\mu + g f^{abc} A^b_\mu A^c_\nu)\, G^{\mu\nu}_a\right) \\ &+ \bar{q}_{cfs}\left(i(\gamma_\mu)_{ss'}(\delta_{cc'}\partial^\mu - igA^\mu_a (t^a)_{cc'}) - \delta_{cc'}\delta_{ss'}m_f\right) q_{c'fs'}. \end{aligned}\tag{1.2}$$

Each quark field is represented by a Dirac spinor q_{cfs}, which is a four-component object ($s = 1,..,4$). The gauge fields, *i.e.* the gluons, are denoted by A^μ_a; they are eight ($a = 1,..,8$) and appear in the definition of the covariant derivative D^μ as well as in the gluon field strength $G^a_{\mu\nu}$. Moreover, the Dirac matrices γ^μ ($\mu = 0,..,3$) and the generators t^a of the $SU(3)_C$ symmetry group appear in Eq. (1.2). The generators form a Lie algebra which is given by the structure constants f^{abc}. Note that the quark color index ($c = 1,2,3$) should not be confused with the index of the structure constants, also denoted by c. The latter is in fact contracted with a gluon field and hence, it runs from 1 to 8. Finally, since there are six flavors, the index f runs from 1 to 6. Depending on the flavor, the quark mass m_f varies. Yet, the strong interaction does not distinguish between flavors, meaning there is only one coupling constant g. In general, gauge bosons A_μ arising from non-abelian $SU(N)$ theories are said to self-interact since their field strength tensor $G_{\mu\nu}$ contains a term proportional to $A_\mu A_\nu$. This is not the case for the photon in QED, which originates from the abelian symmetry group $U(1)$. Intuitively, since photons couple to electric charge, they cannot couple to each other, being neutral. However, photons can interact through *e.g.* loops of charged particles.

QCD exhibits some peculiar features that need to be mentioned. First of all, the coupling constant of QCD ($\alpha_s = g^2/4\pi$) is "running" considerably compared to the QED analogue[4] and in the opposite direction. This means that its value changes drastically depending on the energy scale of the physical process: it gets larger at low energies, to the point that any perturbative expansion breaks down. As a consequence, quarks cease to be the relevant DOF. Instead, they are trapped by the strong force inside the hadrons, that become the appropriate DOF. This phenomenon is referred to as *confinement* [24]. At lower energies, where the perturbative expansion in α_s would diverge, alternative

[4]The running of the QED coupling constant is much less severe in the interval of experimentally accessible energies. More concretely: $\alpha(m_e) \approx 1/137$ while $\alpha(m_W) \approx 1/128$, which amount to roughly a 10% change. On the other hand, in QCD, $\alpha_s(m_p) \approx 0.5$ while $\alpha_s(m_W) \approx 0.1$.

theoretical frameworks must be used. Chapter 2 will explore the powerful option of effective field theories, which are free from any model dependence and produce systematically improvable results. Lattice QCD [25] is another powerful tool that operates at low energies, constituting a promising alternative to the effective field theory approach.

On the other hand, at large energies, α_s gets very small; quarks and gluons asymptotically behave as free particles. Perturbative QCD is the appropriate tool to describe strong interactions between quarks and gluons at high energies where the coupling is small. The proof that Yang-Mills theories, gauge theories based on the special unitary group $SU(N)$, lead to *asymptotic freedom* [26, 27], consolidates the choice of gauging the color $SU(3)$ symmetry, *i.e.* to promote it from global to local. In perturbation theory, the amplitude of a process — from initial to final state — is obtained by summing Feynman diagrams, each representing a perturbative contribution to the transition amplitude. Higher-order terms in α_s become less and less important so that the infinite series can be truncated. This yields a finite, accurate approximation of the full calculation. The degree of accuracy can be increased systematically by including higher-order diagrams.

In general, it is convenient to discuss the strong interaction in three different energy regions. This is because for each of these regions, different DOF are at play. In this thesis I refer to low, intermediate and high energy regions. More specifically they correspond to momenta q in the order of:

- $q \ll 1$ GeV $\longrightarrow$ low energies,
- $q \sim 1$ GeV $\longrightarrow$ intermediate energies,
- $q \gg 1$ GeV $\longrightarrow$ high energies.

At low and at high energies, QCD is understood by means of different theoretical tools. "Understood" in the sense that the physics taking place at those energy scales can be described mathematically and quantitative predictions can be made. However, in the intermediate-energy region, where effective field theories become unreliable and perturbative QCD cannot yet be applied, the understanding of QCD is still very poor. At present, it is not even clear whether the relevant DOF in this regime are hadrons or quarks and gluons. Experimental data are needed to guide the development of theoretical models, which aim at describing the strong interaction in this energy regime. In particular, spin observables turn out to be sensitive probes and should therefore be extracted from data associated with the strong production of baryons. This topic will be explored further in section 4.3.

The $SU(3)$ symmetry group is recurrent in QCD. In fact, approximating the masses of the three lightest quarks to the same value, the QCD Lagrangian becomes invariant under flavor $SU(3)$ transformations. In the limit where only the up and down quarks have identical masses, this global symmetry reduces to flavor $SU(2)$, better known as *isospin* symmetry. Furthermore, the additional global $SU(3)_L \times SU(3)_R$ symmetry is obtained by considering the three lightest quarks as massless. This is called *chiral* symmetry since the corresponding

transformations distinguish between left- and right-handed fields $q_{L/R}$, being indeed not compatible with quark mass terms. The QCD Lagrangian of Eq. (1.1) can be decomposed in terms of right- and left-handed quark fields, acting with the projection operators $P_{L/R} = \frac{1}{2}(\mathbb{1} \mp \gamma_5)$ on the quark fields. The mass term mixes fields with different handedness. The massless part, which includes the quark-gluon interaction, is characterized by a complete separation of left- and right-handed fields. Therefore, it is chirally invariant. The chiral symmetry of QCD is at the basis of the development of the low-energy effective field theory of QCD presented in chapter 2.

The massless QCD Lagrangian is also invariant under the $U(1)_L \times U(1)_R$ chiral symmetry, which is often rewritten in terms of the vector and axial-vector groups, $U(1)_V \times U(1)_A$. All together, the massless QCD Lagrangian possesses the global symmetry:

$$SU(3)_L \times SU(3)_R \times U(1)_V \times U(1)_A \equiv U(3)_L \times U(3)_R.$$

Baryon number conservation is an observable effect of the realization of the $U(1)_V$ symmetry in nature. On the other hand, $U(1)_A$ is only a symmetry at the Lagrangian level, but it is lost in the quantized theory, giving rise to an anomaly [28]. The corresponding axial current is indeed not conserved [29]:

$$\partial_\mu J^\mu_A = \frac{g^2 N}{32\pi^2} \widetilde{G}^a_{\mu\nu} G^{\mu\nu}_a \tag{1.3}$$

where $\widetilde{G}_{\mu\nu} = \varepsilon_{\mu\nu\rho\sigma} G^{\rho\sigma}$ is the dual field strength tensor and N is the number of massless quark flavors. The right-hand side of Eq. (1.3) can be rewritten into a total derivative, suggesting the existence of a new conserved current. However, the corresponding charge is not conserved, because of the topologically non-trivial structure of the QCD vacuum. The QCD Lagrangian of Eq. (1.1) should effectively contain one additional term:

$$\mathscr{L}_\theta = \frac{\theta g^2}{32\pi^2} \widetilde{G}^a_{\mu\nu} G^{\mu\nu}_a, \tag{1.4}$$

known as θ-vacuum term, which respects the underlying gauge symmetry but violates parity and CP symmetry. As a direct implication, the neutron is expected to have a non-zero electric dipole moment. The experimental upper bound on this observable is $2.9 \times 10^{-26} e\,\mathrm{cm}$ [30], which constrains the parameter θ to a very small value. This fine-tuning problem is known as the *strong CP problem*.

1.4.3 CP violation

In the previous sections, the word *symmetry* has been mentioned often, due to its importance in constructing any theory. Not only continuous symmetries,

but also discrete ones like charge conjugation (C), parity (P) and time reversal (T) exist. These operations cannot be achieved combining infinitesimal continuous transformations starting from the identity. In the following, C and P transformations will be investigated in more detail.

Parity flips the sign of the three-momentum of a particle but not of its spin. A parity transformation on spacetime x^μ leads to

$$x^\mu = (t, \mathbf{x}) \longrightarrow \tilde{x}^\mu \equiv x_\mu = (t, -\mathbf{x}).$$

On a Dirac field $\psi(x)$, it is implemented by a unitary operator P such that

$$\psi(x) \longrightarrow P\psi(x)P^{-1} = \eta_P \gamma_0 \psi(\tilde{x}),$$

where η_P is a phase, called intrinsic parity of the field. Since applying this operation twice is equivalent to act with the identity operator, the phase η_P is constrained to ± 1 [31]. Conventionally, and without loss of generality, elementary fermions have positive intrinsic parity while antifermions have negative[5]. The parity of baryon resonances relative to the proton is however not a convention.

Charge conjugation transforms a particle into its antiparticle, without affecting its spin orientation. It is implemented by the unitary operator C as follows

$$\psi(x) \longrightarrow C\psi(x)C^{-1} = -i(\bar{\psi}(x)\gamma^0\gamma^2)^T.$$

It is really useful to know the transformation properties of the five Dirac field bilinears: $\bar{\psi}\psi$, $i\bar{\psi}\gamma^5\psi$, $\bar{\psi}\gamma^\mu\psi$, $\bar{\psi}\gamma^\mu\gamma^5\psi$, $\bar{\psi}\sigma^{\mu\nu}\psi$, since they are the building blocks entering any Lagrangian. A summary can be found in [12].

The violation of the combined CP symmetry is one of the three necessary conditions to explain the excess of baryonic matter in our universe, according to Sakharov [32]. It is conceivable that immediately after the Big Bang, an asymmetry between the number of baryon and antibaryon might have already existed. However it must have been washed out during the inflation phase, resulting in a early universe with null baryon number [33]. This implies that the baryon asymmetry observed today has generated in parallel with the evolution of the universe. Provided that Sakharov's conditions are satisfied, such an asymmetry can indeed be generated dynamically.

For many years CP was thought to be an exact symmetry of nature, until experimental evidence disproved it [34] in 1964. On the other hand, the combined CPT symmetry still holds true according to all observations performed so far. The SM, being a local quantum field theory satisfying Lorentz invariance, has automatically CPT symmetry, according to the CPT theorem [35, 36]. In particular, the electromagnetic interaction conserves C, P and T separately. The strong interaction breaks P, T and therefore also CP via the θ-vacuum term of Eq. (1.4). This term, even if allowed in a gauge theory based

[5] In Srednicki's textbook [13] and many others, $\eta_P = \pm i$ instead.

on $SU(3)_C \times SU(2)_L \times U(1)_Y$, is left out from the SM since a significant observation of strong CP violation is missing. In the SM, CP violation is implemented exclusively via the weak interaction through the Cabibbo-Kobayashi-Maskawa matrix [37]. The amount of CP symmetry violation predicted by the SM alone is however not enough to explain the baryon asymmetry observed in our universe [33, 38]. Chapter 4 will address this problem in greater detail.

1.5 Form factors

In order to gain a deep understanding of the properties of matter, having identified the elementary particles of nature is surely a first good step. The next step is to describe how these elementary particles form composite objects like nucleons and other hadrons. The next level of complexity is given by atomic nuclei, then atoms, then molecules and so forth. In this thesis, we will be concerned with physics at the femtometer scale, *i.e.* 10^{-15} m, roughly the nucleon size.

The electromagnetic interaction is an excellent tool to probe the inner structure of hadrons. A simple interaction involving a photon, an electron and a positron, *i.e.* classically speaking point-like particles, can be easily described by the QED vertex $-ie\gamma^\mu$. The situation is different when a photon couples to a composite object like a hadron, as depicted in Fig. 1.1. Such a vertex, represented by a blob, is conveniently parametrized by functions called form factors (FFs), which are specific to the considered hadron. The FFs parametrize the deviation from point-like behavior and therefore, they contain precious information on the intrinsic structure of a hadron. The FFs are functions of the momentum transfer squared q^2, which means that they can be experimentally addressed in different kinematical regions, based on the choice of the reaction. The notation FFs is used to denote *elastic* FFs, which involve only one type of

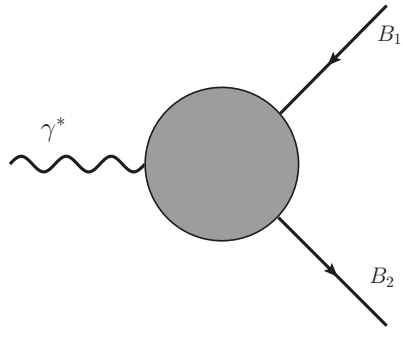

Figure 1.1. Diagrammatic representation of the electromagnetic form factors. If the final baryon is the same as the initial, $B_2 = B_1$, the form factors are called *elastic*. Otherwise they are referred to as *transition* form factors.

hadron, as for $B_2 = B_1$ in Fig. 1.1. In this case, the number of FFs depends on the spin S of the corresponding hadron according to $2S+1$. Less intuitive are the *transition* FFs, in this thesis denoted by TFFs, which involve two different hadrons, *i.e.* $B_2 \neq B_1$. This thesis deals exclusively with TFFs, in particular the two Σ^0-Λ TFFs and the three Σ^{*0}-Λ TFFs. However, some general concepts valid for both FFs and TFFs are discussed below. For pedagogical purposes the simplest case, *i.e.* spin-1/2 baryons only, is taken as an example.

Electromagnetic FFs show up in the transition matrix elements of the electromagnetic current operator $j^\mu = e\bar{q}\mathscr{Q}\gamma^\mu q$, with the quark field $q^T = (u,d,s)$ and the quark charge matrix $\mathscr{Q} = \mathrm{diag}(2/3,-1/3,-1/3)$ [39]:

$$\begin{aligned}\langle B_2|j^\mu|B_1\rangle &= e\,\bar{u}_2\left(\left(\gamma^\mu + \frac{m_1-m_2}{q^2}\,q^\mu\right)F_1(q^2)\right.\\ &\qquad\left.+\frac{i\sigma^{\mu\nu}q_\nu}{m_1+m_2}\,F_2(q^2)\right)u_1\end{aligned}$$

where q^2 denotes the square of the invariant momentum transfer and the photon momentum q_μ is given by the difference between the final and initial baryon momenta. F_1 and F_2 are called Dirac and Pauli FFs. Linear combinations give rise to the Sachs FFs G_E and G_M, called electric and magnetic FFs:

$$\begin{aligned}G_E(q^2) &:= F_1(q^2) + \frac{q^2}{(m_2+m_1)^2}\,F_2(q^2)\,,\\ G_M(q^2) &:= F_1(q^2) + F_2(q^2)\,.\end{aligned}$$

Differential cross section and decay width formulae are often given in terms of the latter since they usually results in simpler expressions, where the electric and magnetic FFs decouple. The absence of cross-terms facilitates their experimental determination. In contrary, interference terms frequently appear when using the Pauli and Dirac FFs.

In the Breit frame ($q^2 = -\mathbf{q}^2$) and for non-relativistic objects[6], the Sachs FFs correspond to the Fourier transform of the charge and magnetization spatial distribution $\rho_{E/M}$. For example, assuming ρ_E to be spherically symmetric,

[6]This requirement is not fulfilled by the hadrons studied in this thesis, which are all relativistic particles. This means that they are light enough to experience recoil due to scattering, *i.e.* their mass does not satisfy $m^2 \gg |q^2|$ for values of $|q^2|$ large enough to resolve the intrinsic structure. The relation between the FFs and the charge/magnetization density distributions is indeed more involved [40].

the following simple relation can be derived, expanding at low energies:

$$\begin{aligned} G_E(q^2) &= \int e^{i\mathbf{q}\cdot\mathbf{r}}\rho_E(r)\,d^3r \\ &\propto \int \rho_E(r)\,r^2\,dr - \frac{\mathbf{q}^2}{6}\int \rho_E(r)\,r^4\,dr + \mathscr{O}(\mathbf{q}^4) \\ &= Q + \frac{q^2}{6}\langle r_E^2\rangle + \mathscr{O}(q^4). \end{aligned} \tag{1.5}$$

At the photon point, *i.e.* $q^2 = 0$, the electric and magnetic FFs, respectively, reduce to the hadron electric charge Q and magnetic moment μ. The electric and magnetic radii $\langle r^2_{E/M}\rangle$ are the first non-trivial quantities in the Taylor expansion. They determine the slope of the respective FF at the photon point.

The quark charge matrix can be decomposed in terms of Gell-Mann matrices λ_a as

$$\mathscr{Q} = \frac{1}{2}\lambda^3 + \frac{1}{2\sqrt{3}}\lambda^8.$$

The first term transforms as an isovector (V) under $SU(2)$ isospin rotations, the second as an isoscalar (S). It follows that even the electromagnetic current can be split in two pieces $j^\mu = j^{\mu,V} + j^{\mu,S}$. Since the octet baryons are grouped in isospin multiplets, *e.g.* the nucleon $N = (p,n)$, the isospin symmetry must constrain the FFs. For example, the proton/neutron FFs are given by the sum/difference of a nucleon isoscalar and isovector part. The dispersive approach developed in Uppsala and introduced in section 3.2 is applicable to purely isovector form factors, *i.e.* those associated with the Σ^0-Λ transition (which are the only ones among spin-1/2 baryons), and the Σ^{*0}-Λ transition (which involve a decuplet baryon). Isoscalar contributions are therefore not addressed within this thesis. A similar work which comprises all members of the baryon octet and therefore must include the respective isoscalar components is [40]. The isoscalar spectral functions suffer from model dependence, being substantially obtained from an empirical parametrization in terms of vector meson exchange.

The FFs are categorized as space- or time-like depending on the sign of q^2, the variable they depend on. By scattering electrons on a fixed target, $e^- B_1 \to e^- B_2$, the transferred q^2 is always negative, which implies that the collected data span exclusively over the so-called space-like region. Traditionally this approach has been adopted to study the nucleon elastic FFs. Eq. (1.5) indicates that the space-like FFs are intimately related to the structure of hadrons. Conversely, the time-like region corresponds to positive q^2. Experimentally this region is explored via Dalitz decays into a lighter baryon and an electron-positron pair and via electron-positron annihilation into a baryon-antibaryon pair. More in detail, the first scenario $B_1 \to B_2 e^+e^-$ gives exclusively access to TFFs in the low-q^2 region, *i.e.* $4m_e^2 < q^2 < (m_1 - m_2)^2$. The second scenario $e^+e^- \to B_1\bar{B}_2$ probes the intermediate-q^2 region, *i.e.*

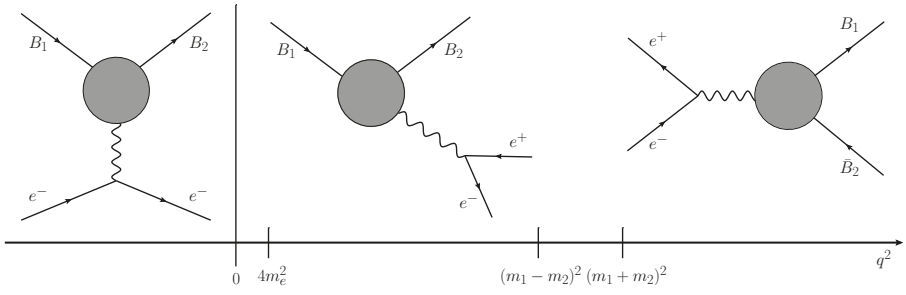

Figure 1.2. Space- and time-like FFs can be accessed exploiting different reactions.

$q^2 > (m_1+m_2)^2$, and applies to both FFs and TFFs since the produced baryon-antibaryon pair can also be composed of particle B_1 and antiparticle $\bar{B}_1$, *i.e.* $m_2 = m_1$. Note that due to these kinematical constraints, some q^2 regions are unaccessible. The diagrams of Fig. 1.2 illustrate which process takes place at each of the three q^2 regions listed above: negative q^2, positive low q^2 and positive intermediate q^2.

At this point it is necessary to make a distinction between the nucleons and the hyperons. The latter are in fact unstable, and therefore not particularly suitable for fixed-target experiments. For hyperons, the space-like region is extremely difficult to cover experimentally. However, this is the region of primary interest from the point of view of hadron-structure studies. A large part of my research focuses on how to retrieve that piece of information, provided that the TFFs are measured at least in the low-energy time-like region, and by means of theoretical tools that will be presented later in sections 2 and 3. Hyperon time-like FFs are a contemporary topic of research: BESIII is already delivering new results in the positive intermediate q^2 region [41]. HADES is addressing TFFs in the positive low q^2 region [42–44]. At a later stage, hyperon-antihyperon pairs will be produced abundantly at PANDA, via proton-antiproton collisions [45,46]. Therefore even PANDA will study TFFs at positive, low q^2.

In the absence of anomalous thresholds[7], both FFs and TFFs are real below the two-pion threshold, *i.e.* for $q^2 < 4m_\pi^2$, and complex above. The existence of an anomalous cut in the complex q^2 plane, with branch point not lying on the real axis, makes the TFFs complex everywhere, even in the space-like region. If the extra branch point lies on the real axis, then the TFFs/FFs are still real below this point. Part of my research has specifically focused on the complications arising when the TFF functions possess anomalous cuts in the complex q^2 plane. At any q^2 point, each TFF is then given by an absolute number and a phase. What matters is the relative phase between the various TFFs, which for hyperons can be directly retrieved from the angular distribution of the decay products. Interestingly, this relative phase is easier to obtain

[7]The definition of anomalous threshold is given in chapter 3.

for hyperons than for nucleons [41]. This topic will be treated in greater detail in Section 4.4.

Unifying forces from the theoretical and experimental side, the long-term goal is to determine *e.g.* the electric charge distribution inside hyperons or in another words to know their TFFs/FFs for any value of transferred momentum square q^2. Comparison with the nucleon FFs will give further insight into the properties of ordinary versus strange matter.

1.6 Scientific questions and achievements

The multipurpose research carried out in this thesis has been "mediated" by hyperon physics. First of all, the study of the electromagnetic and spin properties of the hyperons is interesting per se, being the hyperons the closest relatives of the nucleons. Hyperons (Y), play the role of diagnostic tools in my research, used to address different open questions. At a fundamental level, they reduce to three main ones:

- structure of matter,
- production dynamics in the non-perturbative regime of QCD,
- CP violation.

The experimental complement of this research can be undertaken by means of:

- scattering on hyperons,
- hyperon production,
- hyperon decays.

The interest in the hyperon space-like TFFs comes precisely from the desire to better understand the properties of matter. Scattering reactions, like $e^- Y_1 \to e^- Y_2$ would be perfect to investigate the intrinsic structure of hyperons, such as the electric charge distribution inside these hadrons. However, the hyperons are not suitable targets for scattering experiments, due to their finite lifetime. Other kinematical regions, *e.g.* $Y_1 \to Y_2 e^+ e^-$, have been and will be explored experimentally instead. The question is: with the available theoretical tools and future time-like data, can we predict the behavior of the TFFs in the low-energy space-like region? This motivates papers I and V, where the low-energy isovector TFFs have been studied using a newly developed method, based on dispersion relations, which merge experimental data with theoretical input from chiral perturbation theory. Thanks to dispersion relations, the TFFs can be analytically continued into the experimentally not easily accessible region.

Additional information can be obtained exploiting the weak decays of hyperons, which give easy access to their spin properties. Among the spin observables, the polarization of the parent hyperon can be directly retrieved from the angular distribution of its decay products. The question here is: can we develop a formalism that allows to systematically get the polarization param-

eters directly from the measured angular distributions of the decay products? Paper II contains the derivation of dedicated formulae which aim at retrieving these quantities, similar in spirit to paper IV. The focus of the latter is on the electromagnetic production process $e^+e^- \to Y_1\bar{Y}_2$, related by crossing symmetry to the reactions already mentioned above. In this case, the polarization parameters can be used to study the electromagnetic time-like FFs in the intermediate-energy region. However, hyperons can also be produced via the strong interaction, via $\bar{p}p \to Y_1\bar{Y}_2$, as explored in Paper II. Studying their spin properties, the behavior of the strong interaction at intermediate energies can be investigated. In fact, QCD is not really understood in the energy regime at which these reactions occur. Spin observables are therefore needed to discriminate between theoretical models that describe hyperon production by means of different DOF. Hyperon polarization data, obtained with our formalism, will serve this purpose.

Hyperon weak decays are also a powerful tool to look for violation of CP symmetry. To explain the imbalance between matter and antimatter in our universe, CP violation must occur in larger amount than found so far. It is therefore important to look for new possible sources of CP violation. This information is encoded in the decay asymmetry parameters, which also appear in the angular distribution of the hyperon decay products. The question here is similar to the previous one: can we develop a formalism that allows to systematically get the decay asymmetry parameters directly from the measured angular distributions of the decay products? In order to retrieve all of them, expressions for the full chain of subsequent hyperon decays must be used. Papers II, III and IV are concerned with the derivation of the decay asymmetry parameters in different processes. Moreover paper III estimates the influence of beyond-SM physics via inclusion of a strong CP violating θ-vacuum term.

1.7 Author's contribution

This thesis builds on five papers. My contribution to each paper is summarized below:

Paper I
This paper contributes to a deeper understanding of the structure of matter by studying the electromagnetic TFFs of the Σ^0-Λ hyperons . The initial calculations for this paper were performed by the co-authors. However, some disagreements in the results needed to be solved. My task was to perform all calculations independently in order to establish the correct results.

Paper II
The fundamental questions addressed by this paper are non-perturbative QCD dynamics and CP violation in the baryon sector. I am the sole author of this

paper, which builds on and extends E. Thomé's doctoral thesis [47]. My task was to provide the PANDA collaboration with concrete formulae for the extraction of polarization parameters and decay asymmetry parameters from the reaction $\bar{p}p \to Y_1\bar{Y}_2$.

Paper III
The aim of this paper is to determine the influence of beyond-SM strong CP violation on the Σ^0 decay asymmetry parameter of the $\Sigma^0 \to \Lambda\gamma$ decay. I performed the loop calculations needed to determine the Σ^0-Λ electric dipole moment at leading order of baryon chiral perturbation theory and I wrote the corresponding part in the paper. In addition, I co-supervised a master student, S. S. Nair, working on the rest of this project.

Paper IV
The fundamental topics that motivate this paper are searches for new sources of CP violation and investigation of the structure of matter. Together with A. Kupść, I developed a formalism used to systematically analyze the production and decay chains of baryon-antibaryon pairs produced in e^+e^- annihilation at BESIII. I wrote most of the corresponding sections in the paper and performed the calculations therein.

Paper V
This paper extends the work initiated in paper I and therefore aims at further exploring the intrinsic properties of matter. In particular, I obtained predictions for the low-energy electromagnetic Σ^{*0}-Λ TFFs. I wrote most of the result section, including all tables, plots and their interpretation. In addition, I co-supervised a master student, T. Vitos. First, we obtained various observables such as differential cross section and decay widths in terms of the considered TFFs. Second, we studied the analytic structure of these TFFs and located where their branch points sit on the Riemann sheets. Finally, we concluded that the presence of an anomalous cut definitely needed to be taken into account when formulating dispersion relations for the TFFs. I also calculated the chiral perturbation theory input that enters the Σ^{*0}-Λ TFF dispersion relations, *i.e.* the $\Sigma^{*0}\bar{\Lambda} \to \pi^+\pi^-$ reduced amplitudes, to cross-check the results of another master student, O. Junker.

2. Effective Field Theories

The devil is in the detail.

From an earlier German proverb — *Der liebe Gott steckt im Detail*, which translates as *God is in the detail*.

The crucial point that makes effective field theories (EFTs) effective is to exploit the separation of energy scales that is spontaneously present in nature[1]. Understanding which DOF are excited at a specific energy scale and which are not touched by it is a necessary first step. The relevant DOF are those needed to describe the physics that takes place around that energy scale. Paraphrasing my supervisor: to study the motion of a piece of chalk thrown in the air, it is enough to treat it as a point-like object and to know its mass and initial velocity. There is no need to care about molecules and atoms that compose it. In a similar way, Galilean relativity works beautifully as long as the velocities involved are significantly below the speed of light, but fails when this condition is not fulfilled. Einstein's special relativity recovers the Galilean limit and goes beyond it, to the price of being more complex. A more sophisticated theory of relativity may be developed in the future, yet it will not disprove Galilean relativity within its range of applicability. Depending on the physics of interest, one can smartly choose the most convenient theory, as long as it is appropriate for the given scale. In brief, the chosen level of detail should be adequate for the physics question that one wants to answer.

The EFT scale is usually given by the representative momentum or energy for a specific process. Naturally, the range of applicability of an EFT is limited to a specific energy region; as soon as one goes beyond it, new DOF are excited and the theory becomes incomplete and unreliable. In an EFT, the Lagrangian is given by an infinite tower of terms, *i.e.* interactions. Their importance is given by a so-called power counting scheme, which is based on the scale separation. The power counting is a fundamental ingredient because it allows to systematically neglect less relevant terms at a given order in the expansion. Thanks to counting rules, the infinitely many terms, and therefore parameters in an EFT Lagrangian, are reduced to a finite amount. This results in predictive power. In principle, any quantity computed within an EFT framework, can be

[1] This separation can be artificially enhanced in theory, *e.g.* by taking the chiral and/or large-N_c limit, where N_c denotes the number of colors.

determined to the desired accuracy by taking into account higher-order corrections[2]. In other words, EFTs allow to estimate the error associated with any calculated quantity, by following a well-defined procedure. This is something that phenomenological models cannot offer. EFTs have been widely applied to different branches of particle physics; the interested reader can found more details in [48–50].

2.1 Chiral perturbation theory

The low-energy EFT of QCD is called chiral perturbation theory (ChPT). Gasser and Leutwyler are acknowledged as the main developers of this theory [51, 52]. The original idea was introduced first by Weinberg in 1979 [53]. ChPT has been very successful in studying the non-perturbative aspects of the strong interaction. In the field of low-energy hadron physics it has played a dominant role in shaping our understanding of *e.g.* the static properties of the light mesons and their interactions [54–58]. A quite detailed and pedagogical introduction to the subject is given in Refs. [59, 60], which contain all the material presented in this section and much more.

At low energies, the quarks and gluons are not resolved and therefore, in the spirit of EFT, they should be left out from this framework. The relevant DOF are instead the lowest-lying hadrons, the three (eight) pseudoscalar mesons: $\pi^{\pm}, \pi^0, (K^{\pm}, K^0, \bar{K}^0, \eta)$. These are often called pseudo-Goldstone bosons since they are associated with a SSB[3]. Here "pseudo" refers to the fact that they are not massless. Yet, their mass is well below 1 GeV, the typical hadronic mass scale. This implies that there is a net mass separation between the pseudoscalar octet and the lightest baryons, *i.e.* the nucleons. In the following, I will present few arguments why the pseudoscalar mesons are chosen as fundamental DOF in this EFT. At sufficiently low energies with respect to the chiral symmetry breaking scale ($\Lambda_\chi \sim 1$ GeV), the three heavier quarks can be ignored, or "frozen" DOF. Furthermore, recall from section 1.4.2 that taking the lightest N (2 or at most 3) quarks as massless (chiral limit), the QCD Lagrangian gains an additional global symmetry $SU(N)_L \times SU(N)_R$ called chiral symmetry. The corresponding conserved currents can be reorganized into linear combinations with distinct behavior under a parity transformation: vector and axial-vector currents. There is however no evidence of this symmetry in the observed particle spectrum: parity partners, *i.e.* degenerate spin and mass states with opposite parity, are missing. A possible explanation is that the original symmetry of the Lagrangian has been spontaneously broken, meaning that it is not shared by the ground state. A direct consequence of SSB is the presence of massless Goldstone bosons [22, 61]. These were already

[2]Note that in a EFT, the order of the expansion is not given by the power of the coupling constant.

[3]The SSB of QCD in the chiral limit will be discussed later.

discussed by Nambu in Ref. [62], in the context of condensed matter physics, more precisely superconductivity theory. Looking at the particle spectrum, one finds light pseudoscalar mesons which indeed can be associated with the spontaneous breaking of the axial-vector $SU(N)_A$ symmetry. Their quantum number $J^P = 0^-$ (odd parity) is in agreement with the axial-vector charges corresponding to Noether's conserved currents which originate from the global and continuous symmetry of the massless QCD Lagrangian [63]. Note also that the number of Goldstone bosons originating from the SSB of $SU(N)_A$ is $N^2 - 1$, as the number of generators of that symmetry group. The ground state still possesses the vector $SU(N)_V$ flavor symmetry, reflected by the flavor multiplets of the Eightfold Way. These properties stem from the quark condensate in the chiral limit:

$$\langle 0|\bar{q}q|0\rangle = \langle 0|\bar{q}_L q_R + \bar{q}_R q_L|0\rangle \neq 0$$

which is the order parameter for the spontaneous breaking of the chiral symmetry[4]. Restoration of the chiral symmetry would imply that $\langle \bar{q}q\rangle \to 0$. The quark condensate is obviously not invariant under a chiral transformation, but it is left unchanged by any transformation belonging to the $SU(N)_V$ subgroup, which acts identically on the right- and left-handed fields.

Since quarks are not massless in reality, the chiral symmetry is not exact, but approximate. It is indeed explicitly broken by the small quark masses. Hence, even the Goldstone bosons are massive, yet much lighter than the other hadrons. This constitutes a mass gap that allows for a scale separation. Furthermore, the light quark masses are not identical, meaning that the flavor symmetry is not exact either. Therefore, the hadrons grouped in flavor multiplets are not degenerate in mass, but close to.

As a side note, the $U(1)_A$ anomaly mentioned in section 1.4.2 is restored to a symmetry in the chiral limit if the number of quark colors is taken to infinity, known as the large-N_c limit [64]. Under these circumstances, the additional SSB of $U(1)_A$ implies the existence of one more Goldstone boson, identified as the η' meson. In a large-N_c world, it would be massless. However, in reality its mass is too close to 1 GeV to consider it a Goldstone boson. Only in large-N_c ChPT one can formally include the η' among the Goldstone bosons[5] [65].

To summarize, ChPT is an EFT for the QCD Goldstone bosons. This EFT can effectively replace QCD at low energies, where quark-gluon perturbation theory is not applicable. Depending on whether the chiral limit is extended or not to the strange quark (in addition to the up and down quarks), the Goldstone bosons are given by the full pseudoscalar octet or just the pion triplet. A brief technical section follows below, summarizing how the leading-order (LO) chiral Lagrangian is derived.

[4] In the SM, the order parameter for the breaking of the electroweak symmetry is the vacuum expectation value of the Higgs field.

[5] The η and η' mesons are indeed obtained from the mixing of the non-physical singlet η_0 and octet η_8 states.

2.1.1 Lowest-order ChPT Lagrangian

The guiding principle when building the ChPT Lagrangian is to mirror the properties of the QCD Lagrangian in the chiral limit. Invariance under the symmetry group $SU(N)_L \times SU(N)_R \times U(1)_V$ as well as charge conjugation and parity is a requirement. Moreover, the ground state of ChPT has to break the $SU(N)_A$ symmetry, exactly as for the ground state of QCD. The Goldstone bosons arising from the SSB of chiral QCD must be pseudoscalars transforming as a triplet or an octet under $SU(N)_V$, with N equal to 2 or 3, respectively. For N=3, they are collected in the matrix

$$\phi = \begin{pmatrix} \pi^0 + \frac{1}{\sqrt{3}}\eta & \sqrt{2}\pi^+ & \sqrt{2}K^+ \\ \sqrt{2}\pi^- & -\pi^0 + \frac{1}{\sqrt{3}}\eta & \sqrt{2}K^0 \\ \sqrt{2}K^- & \sqrt{2}\bar{K}^0 & -\frac{2}{\sqrt{3}}\eta \end{pmatrix}.$$

In order to proceed with the construction of the ChPT Lagrangian, it is convenient to introduce the $SU(3)$ matrix

$$U(x) = \exp\left(i\frac{\phi(x)}{F_0}\right), \tag{2.1}$$

where the constant F_0 has the dimension of energy in order to make the argument of the exponent dimensionless. Its numerical value can be retrieved from the weak decay of the charged pion; at LO, $F_0 = F_\pi = 92.4$ MeV, also known as pion decay constant.

Since $U^\dagger U$ gives trivially the identity, the derivative of U has to appear already at LO. The first non-trivial term one can build, respecting Lorentz invariance, is:

$$\frac{F_0^2}{4}\mathrm{Tr}(\partial_\mu U \partial^\mu U^\dagger).$$

Global $SU(3)_L \times SU(3)_R$ chiral transformations

$$U(x) \mapsto RU(x)L^\dagger \qquad R, L^\dagger \in SU(3)$$

leave the Lagrangian unchanged. By expanding the exponential

$$U = \mathbb{1} + i\phi/F_0 + ...,$$

the kinetic term as well as interaction terms will appear.

The small quark masses can be incorporated in the theory, yet preserving chiral invariance. This is achieved by the following trick: an external field X which has to transform as $X \mapsto RXL^\dagger$ is introduced in order to formally replace the quark mass matrix $\mathscr{M} = \mathrm{diag}(m_u, m_d, m_s)$. Subsequently, the following mass term can be added to the LO Lagrangian:

$$\frac{F_0^2 B_0}{2}\mathrm{Tr}(XU^\dagger + UX^\dagger),$$

where B_0 is related to the chiral quark condensate by $F_0^2 B_0 = -\langle 0|\bar{q}q|0\rangle$. At LO, F_0 and B_0 are the only two parameters of ChPT.

The final step is to promote the global chiral symmetry to local. In fact, it is not the QCD Lagrangian, but rather the locally invariant generating functional $Z_{\rm QCD}$ that should be approximated by infinitely many effective ones

$$\sum_n Z_{\rm eff}^{(2n)} \to Z_{\rm QCD}.$$

$Z_{\rm QCD}$ stems from QCD in the presence of the external fields l_μ, r_μ, s, p, which is described by adding the following Lagrangian to the massless one:

$$\mathscr{L}_{\rm QCD}^{\rm ext} = \bar{q}_L \not{l} q_L + \bar{q}_R \not{r} q_R - \bar{q}_R(s+ip)q_L - \bar{q}_L(s-ip)q_R. \tag{2.2}$$

The above is obtained from the Noether currents corresponding to the conserved global chiral symmetry[6] and from the scalar and pseudoscalar quark densities. The external fields are 3×3 matrices in flavor space, *e.g.* $l_\mu = l_\mu^a \frac{\lambda_a}{2}$. Note that the usual QCD mass term of Eq. (1.1) is recovered by replacing $s \to \mathscr{M}$ and $p \to 0$ in Eq. (2.2). In other words, the field X can be written in terms of the scalar s and pseudoscalar p fields as $X := s + ip$. However, in the literature, the field X is usually redefined as $\chi := 2B_0(s+ip)$. In that way, the dimensionality of χ fits to the power counting introduced below in Eq. (2.4).

Meanwhile, in ChPT the Goldstone boson fields will transform according to $U(x) \mapsto R(x)U(x)L^\dagger(x)$, where $R(x)$ and $L(x)$ are $SU(3)$ matrices. The gauge fields $r_\mu(x)$ and $l_\mu(x)$ can be used to compensate for the right- and left-handed spacetime dependent transformations, respectively. The gauge covariant derivative D_μ replaces ∂_μ according to

$$D_\mu U := \partial_\mu U - i r_\mu U + i U l_\mu .$$

Note in passing that thanks to these additional external fields, ChPT can be used to study the electromagnetic interactions of the light pseudoscalar mesons and their semileptonic weak decays. With these building blocks, the most general effective Lagrangian can be built:

$$\mathscr{L}_{\rm QCD}[q, A_\mu, l_\mu, r_\mu, s, p] \to \mathscr{L}_{\rm ChPT}[U, \partial_\mu U, l_\mu, r_\mu, s, p].$$

The first non-trivial terms are of order $\mathscr{O}(q^2)$, where q is a small quantity like the meson soft momenta and masses. These terms constitute the LO:

$$\mathscr{L}^{(2)} = \frac{F_0^2}{4}\left(\mathrm{Tr}(D_\mu U (D^\mu U)^\dagger) + \mathrm{Tr}(\chi U^\dagger + U\chi^\dagger)\right). \tag{2.3}$$

Section 2.1.2 will clarify which power counting has been used, a fundamental ingredient to build the EFT Lagrangian. For the moment note that the superscript 2, indicating the order of the Lagrangian (2.3) in the chiral expansion,

[6] The vector current associated with the $U(1)_V$ symmetry is left out for simplicity. Meson fields transform trivially under $U(1)_V$ because they have zero baryon number.

corresponds to the number of derivatives in the first term. The second term, *i.e.* the quark mass term, must therefore be equally important. Note also that terms containing an odd numbers of Goldstone bosons cannot be built at this order. In fact, as long as a fully chirally symmetric Lagrangian is constructed, they neither appear at the next chiral order. An additional term of order $\mathcal{O}(q^4)$, induced by the chiral $U(1)_A$ anomaly and derived by Wess, Zumino and Witten [66, 67], needs to be added to the ChPT Lagrangian in order to describe *e.g.* the decay $\pi^0 \to \gamma\gamma$.

The parameters of ChPT are called low-energy constants (LECs). In principle, they could be obtained from the underlying, more fundamental theory of QCD, but in practice they cannot be calculated directly from it with present techniques. They are treated as free parameters, which can be estimated by *e.g.* comparison to lattice QCD and/or experimental data. They contain the influence of higher-mass states that are not included in the theory because not resolved at the considered energies. The number of LECs increases drastically with the order of the expansion, which is a disadvantage with respect to a renormalizable quantum field theory. In fact, the EFT has no predictive power as long as the LECs are not fixed.

2.1.2 Power counting

As in all EFTs, a power counting scheme is needed in order to organize the infinitely many Lagrangian terms according to their importance. This makes us able to truncate the series to a desired accuracy and, at the same time, estimate the corresponding theoretical error. The power counting scheme in ChPT builds on the fact that there is a scale separation between the Goldstone bosons and all other hadrons. At least in theory this is obvious since in the chiral limit the Goldstone bosons would be massless, hence a mass gap between pseudoscalar mesons and other hadrons originates. Note however that in the real world (with real physical masses) this net separation is at the edge of applicability, especially when the whole pseudoscalar octet is included in three-flavor ChPT. Though satisfying results can be obtained in this framework, it makes no sense to extend it further to four-flavor ChPT. This is straightforward to understand since the mass of the charm quark is larger than 1 GeV, *i.e.* above the scale where ChPT breaks down.

The dynamical ChPT scale is given by the light pseudoscalar meson masses, denoted in the following by M. Assuming that a given process involves ordinary momenta q of the same order as M, the power counting scheme can be formulated as:

$$U \in \mathcal{O}(q^0), \quad D_\mu \in \mathcal{O}(q^1), \quad M \in \mathcal{O}(q^1), \quad \chi \in \mathcal{O}(q^2). \tag{2.4}$$

Following this prescription, the ChPT Lagrangian can be constructed, order by order, increasing the number of small quantities of order q^n, *i.e.* derivatives

and quark masses. Physical observables are then obtained as an expansion in q/Λ, where Λ stands for the energy scale at which the EFT breaks down, *e.g.* in ChPT, $\Lambda_\chi = 4\pi F_0 \approx 1.2\,\text{GeV}$. The number of terms to be kept is set by the desired level of accuracy, provided that $q \ll \Lambda$.

A more concrete example can help to better grasp the concept. The ChPT Lagrangian is organized as a sum of infinitely many terms, identified by their order d, which is a positive even integer,

$$\mathscr{L}_{\text{ChPT}} = \sum_{d=2,4,..} \mathscr{L}^{(d)}.$$

Each of them produces vertices of the corresponding order. How can we determine the chiral order of a specific diagram? Let us consider an amplitude $\mathscr{A}$ obtained from a Feynman diagram with L meson loops, I internal meson lines and V_d vertices based on $\mathscr{L}^{(d)}$, for simplicity in four dimensions:

$$\mathscr{A} \propto \int (\mathrm{d}^4 q)^L \frac{1}{(q^2)^I} \prod_d (q)^{dV_d}.$$

The chiral dimension of $\mathscr{A}$ is given by the power of the momentum q to which the amplitude is proportional:

$$\begin{aligned} dim(\mathscr{A}) &= 4L - 2I + \sum_d dV_d \\ &= \sum_d (d-2)V_d + 2L + 2 \end{aligned}$$

where the second line follows from the first based on topological arguments. Since $d \geq 2$, it follows that the chiral dimension for a generic ChPT diagram is $dim(\mathscr{A}) \geq 2$. In particular, only a finite number of possible values for L and V_d are allowed for a given chiral dimension $dim(\mathscr{A})$. Moreover, note that for each loop, the chiral dimension is automatically increased by two orders. In the momentum expansion, loop diagrams are therefore suppressed. If loops, *i.e.* corrections, were as important as tree-level diagrams built out of vertices coming from the same order Lagrangian, the expansion scheme and hence the EFT could break down. Therefore, calculations beyond tree-level need special care.

In the presence of loops, ultraviolet divergences arise. Dimensional regularization is used in the first place to separate the finite from the infinite parts. Renormalization then cures the problem by absorbing the infinities in the redefinition of fields and parameters of the bare Lagrangian. In ChPT, all one-loop diagrams built from the LO Lagrangian are of order $\mathscr{O}(q^4)$. The parameters of the next-to-leading order (NLO) Lagrangian, which is also of order $\mathscr{O}(q^4)$, are adjusted to cancel the infinite parts coming from one-loop graphs with vertices of order $\mathscr{O}(q^2)$. Thus, in the mesonic sector, the chiral and loop expansion fit together [51]. The renormalization scheme commonly applied is

the modified minimal subtraction scheme ($\widetilde{MS}$). The bare parameters of the Lagrangian are rewritten in terms of the finite renormalized ones plus so-called counter-terms which cancel the loop divergences and, in this case, also some specific finite pieces.

Using a modified strategy, the octet baryons and even the decuplet (spin-3/2) baryons can be included in the EFT. This extension is extremely important because it permits a broader application within the field of hadron physics. In particular, it is the starting point of all the EFT calculations I performed in my research. In the following, it is explained how such an EFT can be constructed.

2.2 Baryon chiral perturbation theory

The DOF of ChPT are the pseudoscalar mesons, the Goldstone bosons of QCD. Recall that ChPT builds on the separation between the Goldstone boson mass scale and the typical mass of other (heavier) hadrons *e.g.* nucleons. At first, it might seem impossible to construct an EFT which includes baryons, since strictly speaking there is no mass gap to exploit. However, it is indeed possible using a different strategy. This is what baryon chiral perturbation theory (BChPT) does. The prerequisite is that within this framework, the momenta of the Goldstone bosons never become as large as the heavy scale of baryon masses[7]. The material presented in this section follows closely Ref. [60].

2.2.1 Lowest-order BChPT Lagrangian

The goal is to construct a Lagrangian that is able to describe the interactions between the spin-1/2 baryons and the pseudoscalar mesons of ChPT. The octet baryons, represented by four-component Dirac fields, are conveniently collected in a 3×3 matrix

$$B = \begin{pmatrix} \frac{1}{\sqrt{2}}\Sigma^0 + \frac{1}{\sqrt{6}}\Lambda & \Sigma^+ & p \\ \Sigma^- & -\frac{1}{\sqrt{2}}\Sigma^0 + \frac{1}{\sqrt{6}}\Lambda & n \\ \Xi^- & \Xi^0 & -\frac{2}{\sqrt{6}}\Lambda \end{pmatrix}. \tag{2.5}$$

The desired Lagrangian must again be invariant under $SU(3)_L \times SU(3)_R$ transformations. The Goldstone matrix $U(x)$ of Eq. (2.1) is usually replaced by a new field $u(x)$ that satisfies $u^2 = U$. From its transformation properties, a new function $K(L,R,U)$ is defined according to

$$u \mapsto u' = \sqrt{RUL^\dagger} := R\,u\,K^\dagger(L,R,U),$$

[7]This prerequisite does not hold with respect to the heavy masses of the lowest-lying vector mesons, making their inclusion into the EFT very hard, if not impossible [68].

or, equivalently

$$K(L,R,U) := u'^{\dagger} R u = \sqrt{RUL^{\dagger}}^{\dagger} R \sqrt{U}.$$

To ensure invariance under the chiral symmetry group $SU(3)_L \times SU(3)_R$, the various Lagrangian terms are constructed starting from pieces which individually transform as $K...K^{\dagger}$. As in ChPT, a flavor trace of the final objects is taken as the last step. The baryon matrix of Eq. (2.5) transforms as $B \mapsto KBK^{\dagger}$ where $K(L,R,U)$ belongs to $SU(3)$. When considering only the nucleon doublet N, instead of the full octet B, the transformation reduces to $N \mapsto KN$ with $K \in SU(2)$ instead. Another useful object is

$$u_\mu := i\left[u^{\dagger}(\partial_\mu - ir_\mu)u - u(\partial_\mu - il_\mu)u^{\dagger}\right],$$

which as anticipated transforms also as $u_\mu \mapsto K u_\mu K^{\dagger}$.

At lowest order, the Lagrangian is given by [69]

$$\begin{aligned}\mathscr{L}^{(1)}_{\text{BChPT}} &= \text{Tr}(\bar{B}(i\not{D} - m_0)B) + \frac{D}{2}\text{Tr}(\bar{B}\gamma^\mu\gamma_5\{u_\mu, B\}) \\ &\quad + \frac{F}{2}\text{Tr}(\bar{B}\gamma^\mu\gamma_5[u_\mu, B]),\end{aligned} \tag{2.6}$$

where m_0 is the mass of the baryon octet in the chiral limit. The LECs D and F are estimated from experiments to be $D = 0.80$ and $F = 0.46$. The chirally covariant derivative is defined by

$$D^\mu B := \partial^\mu B + [\Gamma^\mu, B]$$

with

$$\Gamma_\mu := \frac{1}{2}\left[u^{\dagger}\left(\partial_\mu - ir_\mu\right)u + u\left(\partial_\mu - il_\mu\right)u^{\dagger}\right].$$

Instead of considering the Lagrangian of Eq. (2.6), which includes the full baryon octet, it is simpler to learn from the two-flavor equivalent. The latter describes the nucleon-pion interaction [69]:

$$\mathscr{L}^{(1)}_{\pi N} = \bar{N}(i\not{D} - m + \frac{g_A}{2}\gamma^\mu\gamma_5 u_\mu)N \tag{2.7}$$

where m is the nucleon mass and g_A is the axial-vector coupling, both in the chiral limit. The LEC g_A is fixed experimentally and is expected to obey the theory constraint $D + F = g_A$.

Note that odd powers of momenta are allowed in Eqs. (2.6) and (2.7), in contrast to the mesonic sector where they are forbidden by Lorentz invariance. So far, everything seems to proceed analogously to the construction of pure ChPT. However, problems arise when loop diagrams are taken into account. The lightness of the pseudo-Goldstone bosons ($M^2 \propto m_q \in \mathscr{O}(q^2)$) is a crucial ingredient in ensuring that loop diagrams in ChPT are always suppressed

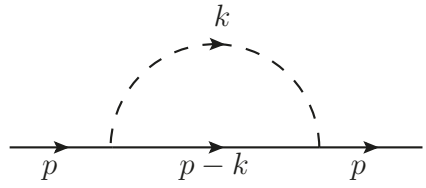

Figure 2.1. One-loop contribution to the baryon self-energy. A baryon/meson line is denoted by a solid/dashed line. Both baryon-meson vertices are $\mathcal{O}(q^1)$.

with respect to tree-level diagrams. If every dimensionful dynamical quantity (momenta, masses) scales in the same way with q, then a simple dimensional analysis of loop diagrams justifies their suppression. This condition is lost when baryons are included, since their masses are not constrained to vanish in the chiral limit. In practice m_0 and m, appearing in Eqs. (2.6) and (2.7), cannot be handled as small quantities since they are close in size to Λ_χ. In addition, the action of the partial derivative ∂_0 on the baryon field is problematic since it gives a large quantity, *i.e.*

$$i\partial_\mu B = p_\mu B, \qquad \text{with} \qquad p_\mu = (m_0, \vec{0}) + (E - m_0, \vec{p}).$$

2.2.2 Power counting

The power counting is modified after the inclusion of the baryons in the EFT:

$$B \in \mathcal{O}(q^0), \quad D_\mu B \in \mathcal{O}(q^0), \quad \mathbb{1}, \gamma_\mu, \gamma_\mu\gamma_5 \in \mathcal{O}(q^0),$$
$$(i\not{D} - m_0)B \in \mathcal{O}(q^1), \quad \gamma_5 \in \mathcal{O}(q^1).$$

The chiral order of a diagram, this time including one baryon line, is given in the following in analogy to section 2.1.2. For an amplitude $\mathcal{A}$ with L loops, V_d meson-meson vertices and $V_{d'}$ meson-baryon vertices, the chiral dimension of $\mathcal{A}$ is:

$$dim(\mathcal{A}) = \sum_d (d-2)V_d + \sum_{d'} (d'-1)V_{d'} + 2L + 1. \tag{2.8}$$

Here d and d' correspond to the order of the underlying Lagrangians and are both positive integers. In addition, d is even. Following the naïve power counting of Eq. (2.8), one-loop contributions should appear first at $\mathcal{O}(q^3)$. However, in practice this does not happen, resulting in a failure of the power counting [69]. As an example, consider the loop diagram of Fig. 2.1, with one meson and one baryon propagator. Such a diagram is calculated to find the one-loop correction to the nucleon mass. In the two-flavor sector, one obtains:

$$m_N = m - 4c_{1r}M^2 - \frac{3g_{Ar}^2 M^2}{32\pi^2 F_{0r}^2} m - \frac{3g_{Ar}^2 M^3}{32\pi F_{0r}^2}, \tag{2.9}$$

where the constants g_{Ar}, c_{1r}, F_{0r} are $\widetilde{MS}$-renormalized. The second term on the right-hand side of Eq. (2.9) is a tree-level contribution to the nucleon self-energy, of order $\mathcal{O}(q^2)$. The LEC c_1 comes from the NLO pion-nucleon Lagrangian which can be found in [69, 70]. The third term is the first loop contribution, surprisingly also of order $\mathcal{O}(q^2)$ and therefore in disagreement with the power counting.

The choice of renormalization scheme plays a crucial role in determining whether the power counting is respected or violated. As shown by Eq. (2.9), in the baryonic sector the $\widetilde{MS}$ scheme alone leads to a violation of the power counting. However, it can be recovered by subtracting an additional finite piece, namely the problematic term mentioned above. In practice, one rewrites $c_{1r} = c_1 + \delta c_1$ and fixes δc_1 so that the nucleon mass at $\mathcal{O}(q^3)$ reads

$$m_N = m - 4c_1 M^2 - \frac{3g_A^2 M^3}{32\pi F_0^2}.$$

This is finally reconciled with the power counting. Observe that these LECs are generally not the same as those of Eq. (2.9) since they are obtained following a different renormalization scheme. The question is: does this operation work in general? Historically, the first remedy to the power counting problem is known as heavy-baryon (HB) ChPT[8] [72, 73]. The basic idea behind HBChPT is to treat baryons as heavy matter fields, whose three-momenta ought to be small, *i.e.* of order $\mathcal{O}(q)$. In the following we consider the nucleon, but the very same strategy applies to the baryon sector in general. The nucleon momentum is separated into a large piece and a tiny one:

$$p_\mu = \underbrace{m v_\mu}_{large} + \underbrace{t_\mu}_{tiny}$$

with the baryon velocity v_μ satisfying $v^2 = 1$, $v_0 \geq 1$ and $v \cdot t \ll m$. The EFT expansion is then organized in increasing powers of $\frac{t}{m}$ and $\frac{t}{\Lambda_\chi}$, *i.e.* in terms of the inverse of both the nucleon mass and the chiral symmetry breaking scale. The nucleon field can also be divided in two pieces, velocity eigenstates, one so-called light component and one heavy:

$$N(x) = e^{-imv\cdot x}(\mathcal{N}(x) + \mathcal{H}(x))$$

obtained acting with the projection operators $P_\pm := \frac{1}{2}(\mathbb{1} \pm \not{v})$. For example $\mathcal{N} = e^{imv\cdot x} P_+ N$ is the light component of the nucleon field. The heavy field $\mathcal{H}$ can be integrated out from the Lagrangian of Eq. (2.7), giving rise to the HBChPT Lagrangian. It is instructive to compare the relativistic LO Lagrangian of Eq. (2.7) with the corresponding HBChPT one:

$$\mathcal{L}_{\pi N}^{(1)} \xrightarrow{HBChPT} \bar{\mathcal{N}}(iv\cdot D + g_A S\cdot u)\mathcal{N} + \mathcal{O}(1/m) \tag{2.10}$$

[8] Formally developed in analogy to heavy-quark EFT, which aims instead at describing bound states of the charm/bottom quark with a light antiquark, *e.g.* B and D mesons [71].

where the spin matrix $S_\mu := \frac{i}{2}\gamma_5\sigma_{\mu\nu}v^\nu$ has been introduced for convenience. The action of the partial derivative on the light nucleon field $\partial_\mu \mathscr{N}$ gives the small momentum t_μ, *i.e.* the derivative in the HBChPT Lagrangian (2.10) is soft. The power counting therefore resembles that of mesonic ChPT:

$$\mathscr{N} \in \mathscr{O}(q^0), \quad S_\mu, v_\mu \in \mathscr{O}(q^0), \quad D_\mu \mathscr{N} \in \mathscr{O}(q^1), \quad u_\mu \in \mathscr{O}(q^1).$$

The nucleon propagator derived from the HBChPT Lagrangian is proportional to

$$\frac{1}{p^2 - m^2} \xrightarrow{HBChPT} \frac{1}{2m}\frac{1}{v\cdot t}\,.$$

This implies that when calculating the one-loop diagram of Fig. 2.1 within this framework, one obtains a result of order $\mathscr{O}(q^3)$, in agreement with the counting rules. Finally, note that the LO Lagrangian (2.10) does not contain the nucleon mass anymore. The mass scale m only shows up as a suppression factor in correction terms needed to ensure reparametrization invariance or Lorentz invariance [74]. At higher orders, these corrections become more and more complicated, compromising the usage of this approach.

Other successful approaches, that have the additional advantage of being manifestly Lorentz invariant, are the extended-on-mass-shell scheme [75, 76] and the infrared regularization of BChPT [77]. They cure the breaking of the power counting by adopting different renormalization/regularization methods. In paper III, the loops are calculated using the infrared regularization scheme, which is introduced briefly in the following. Infrared regularization is a technique that enables systematical splitting of the baryon-meson loop integral into a soft- and a hard-momentum piece. Consider the following integral, again corresponding to the problematic one-loop self-energy graph of Fig. 2.1:

$$H(p^2, m^2, M^2; d) := -i \int \frac{\mathrm{d}^d k}{(2\pi)^d} \frac{1}{[(p-k)^2 - m^2 + i\varepsilon](k^2 - M^2 + i\varepsilon)}\,. \quad (2.11)$$

Convergence of the integral is achieved for $d < 4$. However, for vanishing M (chiral limit) and for $d < 3$, the integral develops an infrared (IR) singularity for small loop momenta k of order $\mathscr{O}(q)$[9]. Since for almost-on-shell baryons the difference $p^2 - m^2$ is $\mathscr{O}(q)$, the IR-singular term is of order $\mathscr{O}(q^{d-3})$. The remaining hard-momentum parts are polynomials that can be absorbed in the available parameters, the LECs. The hard-momentum piece constitutes the so-called regular part of the integral. Performing the calculation at threshold, *i.e.* at $p^2 = (M+m)^2$, one gets [60]:

$$H((M+m)^2, m^2, M^2; d) = \frac{\Gamma(2 - \frac{d}{2})}{(4\pi)^{\frac{d}{2}}(d-3)} \left(\frac{M^{d-3} + m^{d-3}}{M+m} \right).$$

[9] For $d = 3$, the IR singularity shows up only if the baryon is on-shell, *i.e.* $p^2 = m^2$. The integral is otherwise regular.

The above result contains both the IR-singular part and the regular part, respectively proportional to M^{d-3} and m^{d-3}. For fractional d, the regular part can be expanded in terms of non-negative integer powers of $M \in \mathcal{O}(q)$. The failure of the power counting is uniquely attributed to this part. By modifying the renormalization scheme, the regular part can however be moved into the counter-terms. On the other hand, the IR-singular part can be expanded in terms of fractional powers of M, which do not spoil the power counting. Therefore, the general prescription to follow in order to agree with the power counting is to replace the integral of Eq. (2.11) by its infrared part.

The bottom line of this section is that the nucleon doublet or baryon octet (2.5) can be included in two- or three-flavor ChPT, with a renormalization scheme chosen such that the chiral power counting works also for the loop diagrams. This has been utilized in paper III.

2.2.3 Incorporation of spin-3/2 resonances

BChPT extends mesonic ChPT by including the spin-1/2 octet baryons in the EFT. However, other baryons relatively close in mass to the nucleon, can be incorporated as well [78, 79]. These are the spin-3/2 decuplet baryons. Note that in regular BChPT, their effects are encoded in the LECs. Here, on the other hand, the aim is to add them as new propagating DOF. As a consequence, the LECs of the new Lagrangian will have different values compared to the BChPT Lagrangian. In doing so, the hope is to extend the range of validity of the EFT and to learn about the properties of a wider group of baryons. The logic is always the same; new DOF are excited as the energy of a process increases. If these DOF can be systematically included in the theory, *i.e.* if a consistent power counting scheme can be established, then the EFT reliability should be preserved even up to those higher energies.

In general, any quantity Q calculated in this framework is given by an infinite series with increasing powers of q:

$$Q = a_1 q + a_2 q^2 + a_3 q^3 + ...$$

where the coefficient a_i represents the overall factor of order $\mathcal{O}(q^0)$ multiplying the scale-dependent part of order $\mathcal{O}(q^i)$. In order to obtain a finite number, *i.e.* a theoretical prediction for the quantity Q in consideration, this series needs to converge to a certain value. However, this is only achieved if higher-order terms contribute less and less. This means that the larger the a_i, the more limited the range of applicability of the EFT. A large a_i (compared to the others) can be caused by a large LEC, indicating that a new relevant degree of freedom, *e.g.* a resonance R, should be included in the theory instead of being integrated out. In fact, if the resonance is integrated out, one obtains LEC $\sim 1/(m_R - m_N)$. Therefore, one can distinguish two cases: i) $m_R - m_N$ being small and ii) $m_R - m_N$ being not small. If $m_R - m_N$ is small, one might

want to include the resonance explicitly to avoid unnaturally large LECs. In this case, one needs to specify how small this mass difference is, for example it can be reasonable to choose $m_\Delta - m_N \in \mathcal{O}(q)$. If the mass difference is not small, the corresponding LECs are not unnaturally large. Then, there is no reason to include the resonance as a dynamical DOF. On the contrary, this should be avoided as we will see in the following. In the frame where one of the baryons is at rest, the momentum of the pion coming from the resonance decay $R \to N\pi$ is approximately given by:

$$|\boldsymbol{p}_\pi| \sim \underbrace{\sqrt{(m_R - m_N)^2 - m_\pi^2}}_{\mathcal{O}(q^0) \text{ or } \mathcal{O}(q)?} \quad \underbrace{\frac{\sqrt{(m_R + m_N)^2 - m_\pi^2}}{2m_R}}_{\mathcal{O}(q^0)} .$$

If the mass difference is $\mathcal{O}(q^0)$, then this pion momentum is *not* soft[10], which spoils the power counting. However in this case, there is no need to treat the resonance as a dynamical DOF.

The decuplet baryons can be treated as heavy baryons in the same way as the octet baryons in HBChPT. However, since these are relativistic objects, they should be described by a Lorentz-invariant theory. In such a theory, particles with spin $s \geq 1$ cause the emergence of non-physical contributions. Constraints can be imposed in order to eliminate the superfluous DOF. In my work, relativistic Rarita-Schwinger fields [80] are used to describe the spin-3/2 baryons. They are denoted by a vector-spinor T^μ, which is a four-vector field with Dirac fields as components. The vector-spinor must satisfy

$$\gamma_\mu T^\mu = 0,$$
$$\partial_\mu T^\mu = 0,$$

in order to reduce the number of independent complex components from 16 to 8, as it should be to describe a particle and antiparticle of spin-3/2.

Interactions involving a pseudoscalar meson, an octet baryon and a decuplet baryon are contained in the LO chiral Lagrangian [81–83]:

$$\mathcal{L}^{(1)}_{\text{decup}} = \frac{1}{2\sqrt{2}} h_A \, \varepsilon_{ade} \, g_{\mu\nu} \, (\bar{T}^\mu_{abc} \, u^\nu_{bd} \, B_{ce} + \bar{B}_{ec} \, u^\nu_{db} \, T^\mu_{abc}) \tag{2.12}$$

where the coupling constant h_A is fixed from experiment and the decuplet is expressed by a totally symmetric flavor tensor T_{abc}. For example

$$T_{113} = \frac{1}{\sqrt{3}} \Sigma^{*+}, \quad T_{123} = \frac{1}{\sqrt{6}} \Sigma^{*0}, \quad T_{223} = \frac{1}{\sqrt{3}} \Sigma^{*-} .$$

Concerning chiral transformations, the fields transform as:

$$T^\mu_{abc} \to K_{aa'} \, K_{bb'} \, K_{cc'} \, T^\mu_{a'b'c'} .$$

[10] Any extension of ChPT that tries to include vector mesons has to deal with this problem, which will be mentioned again in chapter 3.

In my research, the spin-3/2 Σ^* baryons play a fundamental role. In paper I, the charged baryons are exchanged in the tree-level diagrams $\Sigma^0\bar{\Lambda} \to \pi^+\pi^-$, which are calculated using NLO BChPT. In paper V, the Σ^{*0}-Λ TFFs are studied. Here, the decuplet baryons enter the pion-hyperon amplitude not only as intermediate states but also as initial one. In both paper I and V, the Pascalutsa prescription [82] is used to get rid of additional contact terms coming from the spurious spin-1/2 components. It consists in replacing

$$T^\mu \to -\frac{1}{m_R}\,\varepsilon^{\rho\mu\alpha\beta}\,\gamma_5\,\gamma_\rho\,\partial_\alpha T_\beta$$

where m_R denotes the resonance mass, in this case the mass of the Σ^* resonances. The interactions described by Eq. (2.12) can in fact be written in multiple ways and the consequent discrepancies can be compensated for by NLO and higher-order contact terms. Furthermore, in paper V, also the interaction among two decuplet baryons and a Goldstone boson is relevant. Having already applied the Pascalutsa prescription, the LO interaction term of interest reduces to

$$+\frac{H_A}{2m_R F_\pi}\,\varepsilon_{\mu\nu\alpha\beta}\,\bar{T}^\mu_{abc}\,\partial^\nu T^\alpha_{abd}\,\partial^\beta \phi_{cd}\,.$$

The inclusion of spin-3/2 resonances requires a modification of the BChPT power counting scheme. Several approaches on how to organize the chiral and loop expansion exist [78, 79]. However, further details are not needed for the purpose of this work, since there has been no need to calculate loops containing decuplet baryons within BChPT. The dispersive approach presented in the next section offers a very convenient way of dealing with the numerically most relevant parts of loops. In practice, the calculation of one-loop diagrams involving decuplet resonances will reduce to the computation of simple tree-level scattering amplitudes. In paper III, on the other hand, I have used ordinary BChPT for simplicity. In principle, one could improve the calculation therein by including spin-3/2 resonances.

This chapter has explored ChPT and its extension to the light-baryon sector. There is, however, more to add. So far all other hadronic resonances, close to the mass range of the kaons and the η, have been completely ignored. One example is the light vector meson nonet which contains the ρ, ω, K^* and ϕ meson. These additional DOF pose in turn a new challenge since they cannot be incorporated in the EFT in a straightforward way: they would spoil the power counting by bringing in one more static, hard mass scale which is basically untouched by the chiral limit. At the same time, it is well-known that the vector mesons have a dominant role in all hadron-photon interactions[11]. Therefore, one would like to be able to take their contribution into account. Chapter 3 presents a remedy to this problem.

[11] Vector Meson Dominance is a successful phenomenological model which assumes that all hadron-photon interactions are exclusively mediated by vector mesons [84].

3. Dispersion Relations

It is very hard to make predictions — especially about the future.

Attributed to Niels Bohr, but apparently an old Danish proverb.

As explained in section 2.1, the Goldstone bosons originating from the SSB of the chiral symmetry would be massless in a world of massless quarks. However the up, down and strange quarks have a relatively small, yet non-zero mass, which explicitly breaks this symmetry. It follows that also the Goldstone bosons are massive. In particular, when comparing the average mass of the pseudoscalar pions (138 MeV) or of the kaons (496 MeV) with *e.g.* the ρ vector meson (775 MeV), one notices that the separation between the Goldstone bosons and other hadrons is significantly less pronounced in three-flavor ChPT than in two-flavor ChPT, hence faster convergence for the latter. Strictly speaking the range of applicability of ChPT should have its upper limit below the ρ meson mass, if not even below the lighter σ meson.

It definitely is tempting to construct an EFT for both light pseudoscalar and vector mesons as DOF, with the aim to extend the range of validity above that of pure ChPT. Obviously, the power counting scheme has to be modified in order to account for the inclusion of vector mesons. Several attempts have been made in this direction, however a working power counting scheme has not been found yet, and it is not clear if it exists at all. I advice the interested reader to consult C. Terschlüsen's PhD thesis [85] for a pedagogical introduction to the subject and a complete list of references to previous works. Why are the vector mesons, and in general all meson resonances, more problematic to include in this framework than the baryons? The short answer is that they can decay into Goldstone bosons, *e.g.* $\rho \to \pi\pi$. This makes it very hard, not to say impossible, to trace what happened to the original heavy scale, set by the mass of the mother particle. In fact, the momenta of the decay products cannot all be soft [68]. In BChPT, this problem does not occur since baryon number conservation guarantees the presence of a heavy scale throughout the whole process of interest. The failure of the EFT approach with respect to the inclusion of *e.g.* vector mesons motivates the need for alternative approaches, one of them being dispersion relations [86, 87]. They allow to incorporate precise experimental input into a mathematical framework, obtaining more predictive power than the theory alone. The experimental input complements the theory, encoding *e.g.* the effects of the vector mesons in phase-shift measurements [88, 89].

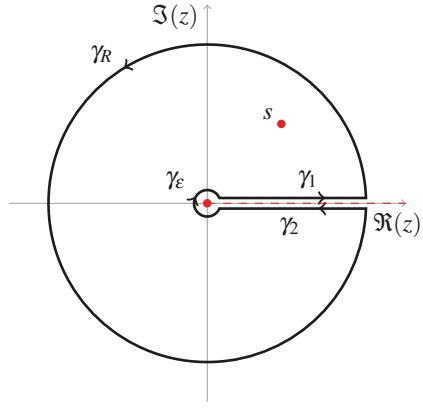

Figure 3.1. The curve γ on which the contour integral (3.2) is defined.

To understand how powerful dispersion relations are, and where they come from, one has to start from the Cauchy theorem. For a function $f : U \subset \mathbb{C} \to \mathbb{C}$ holomorphic in any point of its simply connected domain U, the integral along any closed curve C in U is

$$\oint_C f(z)\,\mathrm{d}z = 0.$$

If the function f is holomorphic in U except for a set of poles z_i of finite order, with $i = 1, .., n$, then the integral is

$$\oint_C f(z)\,\mathrm{d}z = 2\pi i \sum_k Res[f(z)]_{z=z_k} \tag{3.1}$$

where the sum of the residues of the function f runs only over the k poles of f enclosed by the curve C.

Now consider a function $T(z)$, that is analytic in $\mathbb{C} \setminus [0, +\infty)$. From this, we build the function $t(z) = \frac{T(z)}{z-s}$ that has an additional simple pole $z = s$. Here, the choice to have a branch point at $z = 0$ is completely arbitrary. Later, when writing dispersion relations for the TFFs, the branch point will be located at the two-pion threshold $z = 4m_\pi^2$. Regardless, based on Eq. (3.1), the integral of $t(z)$ along a curve γ, which contains the pole $z = s$ and does not cross the positive real axis where the branch cut lies, is equal to

$$\frac{1}{2\pi i} \oint_\gamma t(z)\,\mathrm{d}z = T(s). \tag{3.2}$$

In particular, the contour $\gamma = \gamma_1 + \gamma_R + \gamma_2 + \gamma_\varepsilon$ can be chosen according to

Fig. 3.1, so that the integral of Eq. (3.2) can be rewritten as:

$$\begin{aligned} T(s) &= \frac{1}{2\pi i}\left(\int_0^{+\infty}\frac{T(z+i\varepsilon)}{z-s}\,\mathrm{d}z+\int_{+\infty}^{0}\frac{T(z-i\varepsilon)}{z-s}\,\mathrm{d}z\right) \\ &= \frac{1}{2\pi i}\int_0^{+\infty}\frac{\mathrm{disc}T(z)}{z-s}\,\mathrm{d}z\,, \end{aligned} \tag{3.3}$$

provided that the integrals along the curves γ_R and γ_ε tend to zero as $\varepsilon \to 0$ and $R \to \infty$[1]. Simply by knowing the discontinuity of the function $T(z)$ along the cut $[0,+\infty)$, one can retrieve the value of the function $T(z)$ in any point of its complex domain.

Eq. (3.3) is an example of a dispersion relation. In this simple case where the cut runs exclusively along the real axis, the discontinuity of the function $T(z)$ along the branch cut is related to its imaginary part by $\mathrm{disc}T(z) = 2i\,\mathrm{Im}T(z+i\varepsilon)$. Hence, the dispersion relation is an integral expression which relates the real and imaginary part of the analytic function $T(z)$. Note however that there are functions whose analytic structure is more complicated; when additional cuts appear in the complex plane, away from the real axis, evaluating the function at $z \pm i\varepsilon$ is insufficient. In fact, one wants to evaluate the function to the right and to the left of the cut, following the integration contour along a given direction.

In order to improve the convergence of the dispersion relation for $z \to \infty$, Eq. (3.3) can be rewritten with an extra power of z at the denominator:

$$T(s) = \underbrace{\frac{1}{2\pi i}\int_0^{+\infty}\frac{\mathrm{disc}T(z)}{z-s_0}\,\mathrm{d}z}_{T(s_0)} + \frac{(s-s_0)}{2\pi i}\int_0^{+\infty}\frac{\mathrm{disc}T(z)}{(z-s_0)(z-s)}\,\mathrm{d}z. \tag{3.4}$$

The above is a once-subtracted dispersion relation. The first term is called subtraction constant and might be fixed by experiment. It is a remedy to our incapability of properly treating the higher-energy physics. The second term is less sensitive to the high-energy contribution by a factor $1/z$ with respect to the unsubtracted relation of Eq. (3.3). This is often needed in practice since the imaginary parts of the FFs in the time-like region, *i.e.* the spectral functions $\mathrm{Im}T$, are better known at low energies. If the results obtained from Eq. (3.4) are not satisfactory, the subtraction procedure can be repeated again. This however introduces a new free parameter which reduces the predictive power.

3.1 Optical theorem

Analyticity is the property that makes it possible to write down a dispersion relation. By imposing another fundamental constraint, *i.e.* unitarity, even more

[1]The dispersive approach will be later applied to the TFFs, which are expected to satisfy this requirement.

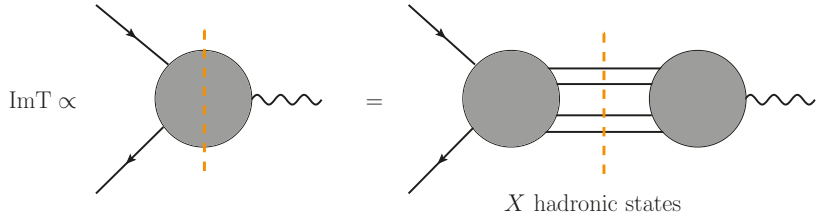

Figure 3.2. A graphic illustration of the optical theorem.

can be achieved. Any reaction in particle physics is characterized by an initial and a final state; the relation between the two is contained in the S-matrix $S = \mathbb{1} + iT$ [12]. Its trivial part, *i.e.* the identity operator, corresponds to the total absence of interaction among the considered initial particles. This implies that the final state will be exactly the same as the initial one. This is always one possible scenario, but something more exciting can happen, too. The T-matrix contains the interesting part, associated with the interactions. No matter how large/small the probability for producing a specific final state is, the sum of all probabilities must give unity. This requirement of probability conservation is achieved by demanding the S-matrix to be unitary:

$$SS^\dagger = \mathbb{1} + i(T - T^\dagger) + |T|^2 = \mathbb{1}.$$

The optical theorem follows directly from the equation above:

$$2\,\mathrm{Im}T = |T|^2 \quad \longrightarrow \quad \mathrm{Im}T_{A\to B} = \frac{1}{2}\sum_X T_{A\to X} T^\dagger_{X\to B}$$

with A and B initial and final states, and X all intermediate states to be summed over. However, in practice one just needs to take into account the most relevant states for X. Fig. 3.2 gives an intuitive picture of what the optical theorem states. As an example, consider the process $\Sigma\bar{\Lambda} \to \gamma^*$. In this case, the two-pion exchange gives the dominant contribution at low energies, since it is the lightest hadronic state that couples to the $\Sigma\bar{\Lambda}$ system. The imaginary part of the $\Sigma\bar{\Lambda} \to \gamma^*$ amplitude can then be obtained by cutting the intermediate pion lines, meaning that the pions are brought on-shell[2]. This implies that the two-pion threshold $z = 4m_\pi^2$ is a branch point from which a cut along the real axis originates. Every additional threshold produces a new cut, making the dispersive approach more involved. Fortunately, as long as only low values of s are considered in Eqs. (3.3) and (3.4), the influence of high-energy inelasticities is suppressed, especially for a subtracted dispersion relation. It is then justified to leave out the loop diagrams where the photon couples to kaons, baryons or more than two pions.

[2]See Cutkosky rules [90]: replace propagator $\frac{1}{p^2-m^2+i\varepsilon}$ by delta function $-2\pi i\,\delta(p^2-m^2)$.

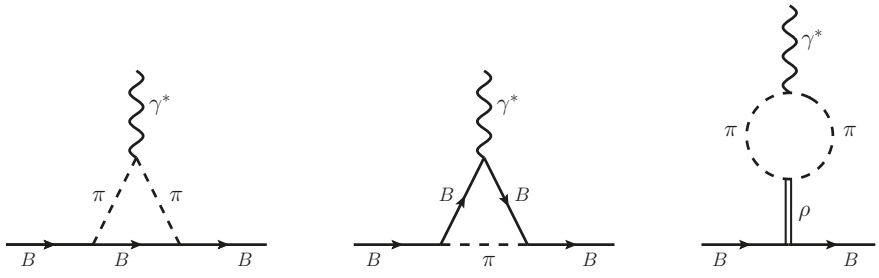

Figure 3.3. One-loop diagrams contributing to the baryon form factors. The letter B stands generically for baryon, not necessarily the same within the same diagram.

3.2 Low-energy form factors of the isovector transition from octet/decuplet to octet baryons

In this thesis, the dispersive approach is presented as a valid tool to determine the low-energy form factors of the isovector transition from octet/decuplet to octet baryons. Nevertheless, it is natural to wonder what can be achieved within BChPT alone [39]. Fig. 3.3 shows the one-loop diagrams that are phenomenologically relevant in the matter of baryon form factors. Only the first two diagrams can be included in BChPT since the third diagram contains a vector meson, namely the ρ. The dispersive framework on the other hand can indeed include the ρ dynamics. This is encoded in the accurate measurement of the pion phase-shift, since the ρ meson is strongly coupled to a two-pion state. This is an advantage with respect to pure BChPT, since vector mesons turn out to be crucial in the description of photon-hadron interactions. The reward for being able to account for this diagram is the extension of the range of validity of the predictions. The first diagram in Fig. 3.3 illustrates the exchange of baryons in the crossed channels, and can be included in the dispersive approach. The exchange of lighter baryons generates left-hand cut structures, while the exchange of very heavy baryons results in polynomial terms. The latter leads to simple contact interactions. In fact, the propagation of a very heavy baryon cannot be resolved. The same holds for the third diagram: the exchange of a heavy vector meson would not be resolved in BChPT and therefore would contribute as a contact interaction. The second diagram is taken care of by the subtraction constant, with corrections being suppressed by $q^2/(4m_B^2)$. The dispersive approach is therefore able to cover all diagrams in Fig. 3.3. In addition, even the complete rescattering of pions can be included via their measured pion phase-shift. In this way, the complete dynamics of the ρ meson is included; in BChPT it would be power expanded as q^2/m_ρ^2, which is not as small as $q^2/(4m_B^2)$.

The hyperon TFFs are analytic functions of $s = q^2$ and therefore expected to satisfy dispersion relations like Eq. (3.3). In the simplest case, their singular-

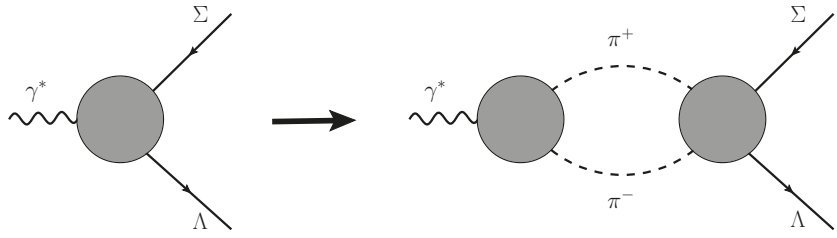

Figure 3.4. The two-pion inelasticity.

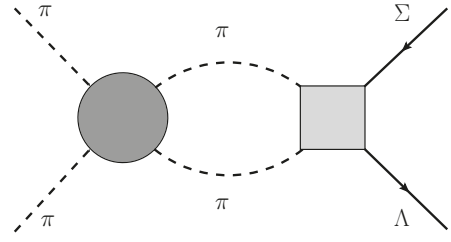

Figure 3.5. Pion-pion rescattering (circle) and pion-hyperon amplitude (box).

ities (poles, branch points) lie on the positive $\Re(z)$ axis[3]. In other words, the TFFs can be written in terms of integrals of their imaginary parts along the cut on the first Riemann sheet, *i.e.* the physical one. In paper I, once-subtracted dispersion relations for the Σ^0-Λ TFFs are given. They provide predictions even for the low-energy space-like region, for which there are no experimental data. Recall from Eq. (1.5) that the space-like region is of interest for the interpretation of the FFs as spatial distributions.

The novel approach developed in Uppsala and presented in paper I builds on the fact that for energies below $\sqrt{s} \approx 1$ GeV, the only inelasticity that comes into play is the one caused by the two-pion exchange shown in Fig. 3.4. This allows to rewrite the imaginary part of the TFFs, $\mathrm{Im}F_i$, in terms of the pion vector form factor F_π^V and the pion-baryon scattering amplitude A_i:

$$F_i(s) = F_i(0) + \frac{s}{12\pi} \int\limits_{4m_\pi^2} \frac{\mathrm{d}z}{\pi} \frac{A_i(z)\, p_{\mathrm{c.m.}}^3(z)\, F_\pi^{V*}(z)}{z^{3/2}\,(z - s - i\varepsilon)}\,. \tag{3.5}$$

Here, $p_{\mathrm{c.m.}}$ is the pion center-of-mass momentum. Note that the scattering amplitude A_i is further decomposed into a part that takes care of pion rescattering and a part that is calculated by NLO BChPT. In Fig. 3.5, these are represented by a circle and box, respectively. The latter is given by the tree-level (Born) diagrams plus NLO contact terms of Fig. 3.6. It turns out that one needs to include the exchange of decuplet resonances in order to produce reasonable

[3] Additional cuts caused by anomalous thresholds do not always lie on the axis. They might appear anywhere in the complex plane.

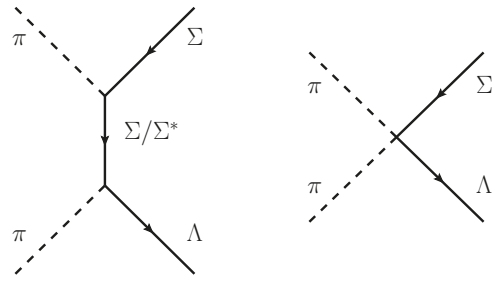

Figure 3.6. LO Born diagrams on the left, *i.e.* hyperon exchange in the t- and u-channel. NLO contact term on the right.

results [91]. The pion-hyperon scattering amplitude of Fig. 3.6 enters our framework as a theory input, in the absence of real data. The crucial contribution of the ρ meson is taken into account by the pion vector form factor, or in other words by the Omnès function

$$\Omega(s) = \exp\left\{ s \int_{4m_\pi^2}^{\infty} \frac{dz}{\pi} \frac{\delta(z)}{z(z-s-i\varepsilon)} \right\} \approx F_\pi^V(s).$$

Here, δ denotes the pion p-wave phase-shift [88, 89], which is experimentally well-known and contains the full information about the dynamics of the ρ meson. The dispersive technique makes it possible to combine the BChPT calculations with experimental data. This is turn allows for retrieving the behavior of ImF_i above the typical EFT energies, up to the vector meson mass region. The accuracy of these predictions is limited by the poor knowledge of a LEC of the NLO BChPT Lagrangian, but will be tremendously increased when more time-like data will be available from *e.g.* HADES and PANDA. In fact, as shown in paper I, this LEC is related to the magnetic transition radius $\langle r_M^2 \rangle$, that can be measured from the slope of the magnetic TFF at the photon point.

As a natural step forward, paper V contains a study of the three Σ^{*0}-Λ TFFs. Here a complication is caused by the Σ^* being unstable with respect to the strong interaction. Since the decay $\Sigma^* \to \Sigma\pi$ is allowed, an additional, so-called anomalous cut will appear on the first Riemann sheet. This cut is induced by the exchange of the octet Σ in the triangle diagram of Fig. 3.7. This baryon is sufficiently light to fulfill the anomalous threshold condition [92]:

$$m_{exc}^2 < \frac{1}{2}(m_{\Sigma^*}^2 + m_\Lambda^2 - 2m_\pi^2),$$

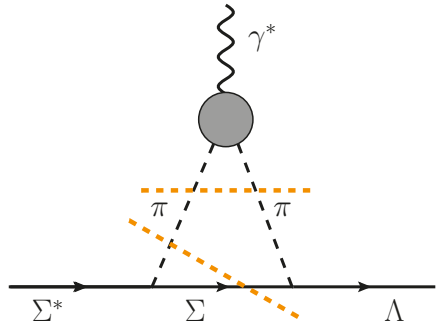

Figure 3.7. Triangle-loop diagram contributing to the electromagnetic Σ^{*0}-Λ TFFs. Beside the unitarity cut, even the anomalous cut caused by the exchange of the Σ hyperon is highlighted in orange.

with m_{exc} the mass of the exchanged particle, in this case the ground-state Σ[4]. Concretely it means that for this particular configuration of internal and external masses, the exchanged Σ-π pair can be on-shell and therefore contribute to the imaginary part of the triangle diagram. As a consequence, the Σ^*-Λ TFF dispersion relations have to be modified accordingly in order to produce correct results. This means that the contour integration path has to circumnavigate the new cut in addition to the familiar two-pion cut. Another consequence is that all three TFFs are complex for any q^2, resulting in a larger number of parameters. The current data situation does not allow for a full determination of the subtraction constants; unsubtracted dispersion relations were used to make predictions in this case.

Thanks to dispersion relations combined with the optical theorem, one has then access to the TFFs in the whole low-energy region, where the effect of other possible, higher-energy inelasticities is suppressed and can be neglected. Dispersion relations allow to bridge between time- and space-like regions in a formidable way. In section 1.5, it was already mentioned that the unstable nature of hyperons makes the experimental determination of their space-like TFFs unfeasible. On the other hand, more and more low-energy, time-like data will be soon available. These are like fuel for our engine, the dispersive machinery, which performs an analytic continuation of the TFF functions into the space-like domain, *terra incognita* so far.

[4]The heavier Σ^*, which can also be exchanged in the same diagram, does not give rise to an anomalous cut.

4. Hyperon Polarization Parameters and Decay Asymmetries

Mathematics is the science of patterns, and nature exploits just about every pattern that there is.

Ian Stewart

Even without polarized beam or target, the hyperons produced via the annihilation of e^+e^- or $\bar{p}p$ are polarized. This polarization can be measured without explicit spin measurements of the final states, a property that has a deep origin, and is the consequence of two crucial ingredients. First, the production process needs to populate more than one partial wave in order to create an interference, which is what polarizes the hyperon. Second, the decay needs to produce an additional overlap of partial waves, in order to preserve the previous interference, *i.e.* the polarization. In brief, the interference pattern of the first process produces a non-vanishing polarization, but it is the decay that reveals this information. As mentioned earlier, most ground-state hyperons decay via the weak interaction. These parity violating decays come with a great advantage: the interference of parity violating and conserving amplitudes gives rise to an anisotropic distribution of their decay products. This unique property allows for direct extraction of decay asymmetry parameters and polarization parameters, without employing a polarimeter. Therefore the hyperons are said to be characterized by *self-analyzing* decays. To introduce these quantities consider a simple example: the weak decay $\Lambda \to p\pi^-$. The angular distribution of the decay products obeys a simple rule [93]:

$$I \propto (1 + \alpha_\Lambda \boldsymbol{P} \cdot \hat{\boldsymbol{n}}_p) \tag{4.1}$$

where α_Λ is the decay asymmetry parameter associated with this specific Λ decay, $\boldsymbol{P}$ is the Λ polarization vector and $\hat{\boldsymbol{n}}_p$ is the unit vector along the direction of the final proton. The decay parameter is defined as

$$\alpha_\Lambda := 2\mathrm{Re}(T_s^* T_p)$$

with T_s and T_p denoting the amplitudes of the s- and p-wave associated with the $\Lambda \to p\pi^-$ decay, satisfying the normalization condition $|T_s|^2 + |T_p|^2 = 1$.

A more complicated example would include a full chain of subsequent weak decays, giving rise to fully differential angular distributions which contain additional decay asymmetry parameters. For example, when looking at $\Omega \to \Lambda K$,

$\Lambda \to p\pi$, three asymmetry parameters would manifest themselves, provided that the whole chain of decays has been included:

$$\begin{aligned} \alpha_\Omega &:= 2\mathrm{Re}(T_p^* T_d) \\ \beta_\Omega &:= 2\mathrm{Im}(T_p^* T_d) \\ \gamma_\Omega &:= |T_p|^2 - |T_d|^2. \end{aligned} \tag{4.2}$$

These asymmetry parameters satisfy $\alpha_\Omega^2 + \beta_\Omega^2 + \gamma_\Omega^2 = 1$. The fully differential angular distributions can be directly fitted to high-statistics data, giving access to more information with respect to the partially integrated ones.

The whole story is indeed more general. What I have been and I will be referring to as polarization here is indeed nothing but an asymmetry parameter. Whenever (at least) two processes that individually have more than one partial wave follow each other, the angular distribution of the final products will display the respective interferences. This chapter contains several examples, of very different nature, but where this very same logic applies. For example:

- strong production + weak decay $\bar{p}p \to \bar{\Lambda}\Lambda$, $\Lambda \to p\pi^-$ + c.c.,
- sequential weak decay $\Omega \to \Lambda K$, $\Lambda \to p\pi^-$,
- electromagnetic production + weak decay $\gamma^* \to \bar{\Lambda}\Lambda$, $\Lambda \to p\pi^-$ + c.c.,
- electromagnetic decay + weak decay $\Sigma^0 \to \gamma\Lambda$, $\Lambda \to p\pi^-$.

In my research I have contributed to develop a systematic method to retrieve both polarization and asymmetry parameters. This terminology distinguishes the first, related to the production process, from the second, related to the decay. As shown by Eq. (4.1), they together appear in angular distributions of hyperon decay products, and are interesting quantities for different reasons. In fact they serve different purposes, and are completely independent of each other.

Regarding the polarization observables, the type of information one is after depends on whether the strong or the electromagnetic force mediates the hyperon production. This is dictated by the type of initial particles involved in the reaction; for example proton-antiproton in paper II and electron-positron in paper IV. Note that the extraction of the polarization observables is performed in the same way regardless of the differences in the production mechanism; it is always conveyed by the hyperon decays.

The decay asymmetry parameters are used instead to construct observables that test CP symmetry. CP violation has been observed in the meson sector, *e.g.* in neutral kaon and B meson decays, recently also in charmed D meson decays. The review *CP violation in the quark sector* in [93] contains a long list of references corresponding to numerous observations, in chronological order. On the other hand, in the baryon sector the only confirmed hint of CP violation originates from the four-body decay of the bottom Λ_b hyperon [94]. It is important to underline that all these observations are in agreement with the SM predictions and therefore insufficient to solve the baryon asymmetry problem, as mentioned in section 1.4.3. Considering the large production rates of

self-analyzing hyperons at ongoing and future experiments, the search for CP violation in baryon decays will continue to be actively pursued in the coming years. Before going into the details of my work, the following two sections give a brief introduction to the density matrix formalism and to the Wigner functions [95], which have been extensively used in papers II and IV.

4.1 Spin density operator

Density matrices are quantum mechanics tools. In quantum mechanics, a physical state is represented by a so-called ket, a state vector $|\alpha\rangle$ in a complex vector space. However, in most experiments, the physics of interest cannot be described by a pure ensemble of identical states. This is simply not how nature works. Instead, density operators are used to represent statistical (incoherent) mixtures, which are more realistic and therefore allow for meaningful predictions. In a mixed ensemble, fractions ω_i of the members can be grouped in pure sub-ensembles, respectively characterized by the same ket $|\alpha^{(i)}\rangle$. The sum over all fractions must give unity. The density operator ρ is defined as:

$$\rho := \sum_i \omega_i |\alpha^{(i)}\rangle\langle\alpha^{(i)}|$$

and by definition contains all the relevant information about the corresponding ensemble. Note that the density operator is Hermitian and must satisfy $\mathrm{Tr}(\rho) = 1$. The expectation value of an observable A, when measurements are carried on a mixed ensemble, is:

$$\begin{aligned}\langle A\rangle :=& \sum_{b'}\sum_{b''}\langle b''|\rho|b'\rangle\langle b'|A|b''\rangle \\ =& \mathrm{Tr}(\rho A).\end{aligned}$$

More concretely, the hyperons produced in *e.g.* $\bar{p}p$ or e^+e^- annihilation processes can be described by spin density matrices, whose dimensions depend on the spin of the particle in consideration. These matrices are expressed in terms of polarization parameters and are obtained from linear combinations of independent Hermitian matrices [96, 97]. For example, for a spin-1/2 particle, the three Pauli matrices $\boldsymbol{\sigma}$ constitute the basis and then there are three polarization parameters: P_x, P_y, P_z. Concretely, the density matrix for a spin-1/2 mother particle can be written as:

$$\rho_{1/2} = \frac{1}{2}\sum_\mu P_\mu \sigma_\mu, \tag{4.3}$$

where σ_0 is the identity matrix, P_0 corresponds to the cross section term and P_i are the components of the polarization vector $\boldsymbol{P}$. Furthermore, the nature of the interaction governing the process of interest might provide additional

constraints on the spin density matrix. The strong force requires parity conservation, which results in two out of these three polarization parameters being equal to zero, namely those components of $\boldsymbol{P}$ that lie in the production plane.

4.2 Wigner functions

For the sake of clarity, I will accurately list the conventions chosen in this thesis, mainly following Ref. [95]. It can be helpful to start from the familiar rotations in three dimensions, which are represented by 3×3 real, orthogonal matrices, here denoted by *e.g.* $R_z(\varphi)$. They act on standard three-component vectors. Any rotation is defined by a rotation axis and the magnitude of the rotation angle. Throughout this thesis, rotation operations act on the physical system actively, leaving the coordinate axes untouched. A positive rotation angle corresponds to a counterclockwise rotation, as seen from the positive side of the rotation axis.

In a quantum mechanics framework, rotations are performed by means of a rotation operator, denoted by $\mathscr{D}(R)$, whose matrix representation will be studied in the following. Depending on the dimensionality of the considered ket space, the order of the square matrix representing the operator $\mathscr{D}(R)$ will vary. A finite rotation about the direction given by a unit vector $\hat{\boldsymbol{n}}$ can be seen as the result of subsequent infinitesimal rotations, by a angle $d\varphi$, generated by the angular momentum operator $\boldsymbol{J}$ according to:

$$\mathscr{D}(\hat{\boldsymbol{n}}, d\varphi) = 1 - i \left(\frac{\boldsymbol{J} \cdot \hat{\boldsymbol{n}}}{\hbar} \right) d\varphi.$$

For instance, choosing the z-axis as rotation axis, a finite rotation by an angle φ is achieved by acting on a ket state with

$$\mathscr{D}_z(\varphi) = \exp\left(\frac{-i J_z \varphi}{\hbar} \right).$$

The order in which rotations about different axes are performed matters, or in other words, the rotation group is non-abelian:

$$[J_i, J_j] = i\hbar \varepsilon_{ijk} J_k. \tag{4.4}$$

The commutation relations of Eq. (4.4) are also satisfied by the intrinsic angular momentum operator $\boldsymbol{S}$, which generates rotations in the abstract spin-1/2 ket space. The spin operator is represented by the Pauli matrices $\frac{\hbar}{2}\boldsymbol{\sigma}$. A spin-1/2 system is represented by a two-component spinor, *i.e.* a column vector. It follows that the rotation operator for spin-1/2 must act on this object as a 2×2 matrix:

$$exp\left(\frac{-i\,\boldsymbol{\sigma} \cdot \hat{\boldsymbol{n}}\, \varphi}{2} \right) = \mathbb{1} \cos(\varphi/2) - i\,\boldsymbol{\sigma} \cdot \hat{\boldsymbol{n}} \sin(\varphi/2).$$

Orthogonal 3×3 matrices can be easily combined to describe a chain of rotations in three-dimensional space. In particular a rotation about an arbitrary axis can always be achieved by performing three rotations, the so-called Euler rotations, around the fixed z- and y-axis:

$$R(\alpha,\beta,\gamma) := R_z(\alpha)R_y(\beta)R_z(\gamma).$$

The quantum mechanics analogue is a product of rotation operators:

$$\mathscr{D}(\alpha,\beta,\gamma) = \mathscr{D}_z(\alpha)\mathscr{D}_y(\beta)\mathscr{D}_z(\gamma),$$

whose matrix representation for $j = \frac{1}{2}$ is:

$$\begin{aligned}
&\exp\left(\frac{-i\,\sigma_3\,\alpha}{2}\right)\exp\left(\frac{-i\,\sigma_2\,\beta}{2}\right)\exp\left(\frac{-i\,\sigma_3\,\gamma}{2}\right)\\
&\quad= \begin{pmatrix} e^{-i(\alpha+\gamma)/2}\cos(\beta/2) & -e^{-i(\alpha-\gamma)/2}\sin(\beta/2) \\ e^{i(\alpha-\gamma)/2}\sin(\beta/2) & e^{i(\alpha+\gamma)/2}\cos(\beta/2) \end{pmatrix}.
\end{aligned}$$

The matrix elements of the rotation operator, for $j = \frac{1}{2}$ or higher,

$$\begin{aligned}
&\mathscr{D}^{j}_{m'm}(\alpha,\beta,\gamma)\\
&= \langle j,m'|\exp\left(\frac{-iJ_z\,\alpha}{\hbar}\right)\exp\left(\frac{-iJ_y\,\beta}{\hbar}\right)\exp\left(\frac{-iJ_z\,\gamma}{\hbar}\right)|j,m\rangle\\
&= e^{-i(m'\alpha+m\gamma)}\langle j,m'|\exp\left(\frac{-iJ_y\,\beta}{\hbar}\right)|j,m\rangle
\end{aligned}$$

are called Wigner functions.

Having introduced these fundamental quantum mechanics tools, it is time to take a closer look at the achievement of my work. The following three sections give an overview of paper II, IV and III, respectively.

4.3 Strong production

The polarization parameters are of great relevance in view of the upcoming PANDA experiment [45], where hyperon pair production will be exclusively mediated by the strong interaction in proton-antiproton collisions [47, 98]. This intermediate-energy experiment will operate at a center-of-mass energy between 2 and 5.5 GeV, posing itself as a unique opportunity to shed light on the behavior of the strong interaction in the non-perturbative domain.

Spin observables like polarization parameters are more sensitive than *e.g.* cross sections to the physics lying behind the production of strangeness in strong processes. The more of the spin observables available, the higher the power to discriminate between various production models which contain different DOF and physics. In the late 1990s several models were proposed,

none of them in agreement with the polarization measurements performed by PS185 at LEAR [99]. These models describe the mechanism of hyperon pair production (specifically $\Lambda\bar{\Lambda}$) starting from the annihilation of strangeness-free baryons like the protons, and give prediction for the expected polarization observables. Different scenarios are considered, from strange meson exchange to quark-gluon models, each leading to quite distinct predictions [100–102].

The reason why precise polarization measurements are needed is twofold. First, data are essential to guide the improved model building, for example by studying how the polarization observables depend on the strangeness content of the final state, *e.g.* $\Lambda\bar{\Lambda}$, $\Xi\bar{\Xi}$ or $\Omega\bar{\Omega}$. At the same time, the LEAR results have to be cross-checked.

An efficient way of retrieving polarization parameters, even for spin-3/2 particles like the triple-strange Ω^- hyperon, is presented in paper II. At the moment there are no corresponding polarization data available. PANDA will fill this gap, and reach much higher statistics for *e.g.* the double-strange Ξ hyperon and single-strange Λ. Paper II focuses specifically on the Ω^- baryon, produced in a PANDA-like scenario. The corresponding 4×4 spin density matrix ρ_{in} must respect the parity symmetry that characterizes the strong production mechanism. It follows that only seven out of its fifteen polarization parameters are non-zero. Note that for spin higher than 1/2, the so-called polarization parameters generalize the three-component polarization vector $\boldsymbol{P}$.

Within the spin density matrix formalism one can systematically implement decay processes, for example $\Omega \to \Lambda K$ and subsequently $\Lambda \to p\pi^-$, by acting with the respective transition matrix T on the initial spin density matrix, $\rho_{\text{fin}} = T\rho_{in}T^\dagger$. Each transition matrix entry $T_{\kappa,\lambda}$ is written in terms of the allowed partial wave amplitudes and Wigner functions, which contain the angular information about the distribution of the decay products. Following Jacob and Wick [103],

$$T_{\kappa,\lambda} \propto \mathscr{D}^{J*}_{\kappa,\lambda}(\phi,\theta,0)B_\lambda$$

where B_λ denote the *helicity* amplitudes with $\lambda = -J,..,+J$. These in turn are related to the *canonical* amplitudes T_L by Clebsch-Gordan coefficients:

$$B_\lambda = \sum_L \left(\frac{2L+1}{2J+1}\right)^{1/2} (L,0;S,\lambda|J,\lambda)T_L,$$

where L refers to orbital angular momentum, *e.g.* $L = 0 \to T_s$.

The angular distribution of the decay products is obtained by taking the trace $\text{Tr}(\rho_{fin}) = \text{Tr}(\rho_{in}T^\dagger T)$. The matrix product $T^\dagger T$ gives rise to interferences between parity violating and conserving amplitudes, which are conveniently encoded in the decay asymmetry parameters α, β, γ of Eq. (4.2).

4.4 Electromagnetic production

The annihilation of an electron-positron pair into a hyperon-antihyperon pair is mediated by the electromagnetic interaction. This process is better understood than the above mentioned $p\bar{p} \to Y\bar{Y}$. Spin density matrices for a process like $e^+e^- \to B_1\bar{B}_{1,2}$ with spin-1/2 baryons have been previously derived in several ways [104–107].

In paper IV the helicity formalism of Jacob and Wick [103] has been used to consider the production of baryons of higher spin and their decay chains. However, for pedagogical reasons I consider here the simplest case, starting from a system of two spin-1/2 particles. Their spin density matrix is given by the following 4×4 matrix:

$$\rho_{1/2,\overline{1/2}} = \frac{1}{4} \sum_{\mu,\bar{\nu}} C_{\mu\bar{\nu}}\, \sigma_\mu \otimes \sigma_{\bar{\nu}}, \tag{4.5}$$

where $\mu = 0, x, y, z$ and $\bar{\nu} = 0, \bar{x}, \bar{y}, \bar{z}$ denote respectively the helicity frames[1] of baryon and antibaryon. The coefficients $C_{\mu\nu}$ depend on the baryon production angle. The electromagnetic production of the baryon-antibaryon pair is mediated by a single photon in our approximation. If the pair consists of spin-1/2 baryons only, as in the case considered here, the number of possible independent helicity transitions is two. It follows that the expressions for $C_{\mu\nu}$ will contain two FFs, *e.g.* the electric and magnetic FFs introduced in section 1.5. Besides the overall strength that enters the cross section, the FFs can be rewritten in terms of two real parameters, one of them being the relative phase between the FFs.

Note how the $C_{\mu\nu}$ coefficients are tightly linked to the polarization parameters introduced in the beginning of chapter 4.1; if the antibaryon is not measured, *i.e.* its spin properties are not resolved, the following *inclusive* density matrix is obtained from Eq. (4.5):

$$\rho_{1/2} = \frac{1}{2} \sum_{\mu} C_{\mu 0} \sigma_\mu .$$

In other words, by comparison with Eq. (4.3), one can identify $C_{00} = P_0$ and $C_{i0} = P_i$ with $i = x, y, z$. The polarization $\boldsymbol{P}$ of this spin-1/2 baryon has been caused by the interference of the electric and magnetic FFs. Since the electromagnetic interaction conserves parity, if *e.g.* the production reaction takes place in the xz-plane, the only non-zero polarization parameter will be $C_{y0} = P_y$.

Regarding the hyperon decays instead, an equivalent[2] description to that of paper II is presented in paper IV. In brief, the action of the transition matrices

[1] Paper IV contains a detailed explanation on how the helicity frames have been chosen.

[2] However, the decay asymmetry parameters have been defined following different conventions. In paper II, PDG conventions were adopted. To be in agreement with [103] and paper IV, T_p should be everywhere in paper II replaced by $-T_p$ (same holds for T_d).

T is replaced by decay matrices $a_{\mu\nu}$ and $b_{\mu\nu}$. To understand the similarities between the two approaches, recall from Eq. (4.3) the density matrix for a spin-1/2 mother (m) particle. The decay into a spin-1/2 and a spin-0 particle can be formally achieved by rewriting

$$\sigma_\mu^m \to \sum_{\nu=0}^{3} a_{\mu\nu}\sigma_\nu^d$$

where, in performing this action, the frame of reference has changed from the initial mother helicity frame to the daughter (d) helicity frame. This procedure can be iteratively implemented for any further step in the decay chain, and it can be extended to initial particles with higher spin in a straightforward way. The T matrix describing the decay of a spin-1/2 baryon into a spin-1/2 and a spin-0 particle in paper II can be related to the matrix $a_{\mu\nu}$ of paper IV by:

$$a_{\mu\nu} = \frac{1}{2}\mathrm{Tr}(T\sigma_\mu^m T^\dagger \sigma_\nu^d).$$

The matrix $b_{\mu\nu}$ instead describes the decay of a spin-3/2 baryon into a spin-1/2 and a spin-0 particle. Expressions for fully differential angular distributions are easily constructed by combining modular expressions corresponding to each decay. Then again, the decay parameters can be determined by fit to data, allowing searches for CP violation in the baryon sector. And the polarization observables can be extracted as well.

The BESIII experiment is copiously producing $e^+e^- \to \bar{Y}Y$ events in order to investigate the time-like FFs and TFFs of various hyperons. Considering fully differential angular distributions, the relative phase among these complex FFs can be retrieved. As shown, this information is contained in the hyperon polarization. It is still a matter of discussion in the hadron physics community what physics content is carried by this energy-dependent observable. Currently very few data points are available, but the long term goal is to study how the phase varies as a function of the transferred energy, with the prospects to infer something more on the hyperon structure [41, 108, 109].

4.5 Electroweak decay

Peculiar is the fact that, contrary to the expectations, there has been no significant observation of CP violation on behalf of the strong interaction. From a theory point of view, a CP violating term can and should be added to the QCD Lagrangian without breaking gauge invariance, as mentioned in section 1.4.2. However, experimental evidence suppresses it to an unnaturally small level. In paper III, a simple extension of regular QCD is considered, by introducing a CP violating θ-vacuum term, and allowing therefore for a somewhat larger amount of CP violation as compared to the traditional SM. This choice produces an electric dipole moment (EDM) for all the baryon octet [110] and also

a Σ^0-Λ electric dipole transition moment (EDTM). The latter is calculated at LO in paper III, and thanks to the existing upper limit on the neutron EDM, also a numerical estimate is obtained. A non-zero EDTM concretely manifests itself in the anisotropic distribution of the Σ^0 decay products, being this again a sign of parity violation. In other words, the EDTM can be related to a decay asymmetry parameter. The three-body decay $\Sigma^0 \to \gamma p \pi^-$, together with the corresponding anti-process, become therefore a tool to look for CP violation. The decay is indeed the result of a two-step decay chain: first the electromagnetic decay $\Sigma^0 \to \Lambda\gamma$ — modified by strong CP violation, then the weak decay $\Lambda \to p\pi^-$. Parity violating and conserving amplitudes originate separately from each of the two decays and their interference shows up in the angular distribution of the final decay products. In particular the asymmetry associated with the first decay is not washed out by the second, thanks to its parity-violating nature. The initial information is then preserved and propagated through, making this specific process an excellent channel to look for baryonic strong CP violation. Since the intermediate Λ hyperon is long-lived, the single-differential decay rate can be decomposed as:

$$\frac{d\Gamma_{\Sigma^0\to\gamma p\pi^-}}{d\cos\theta} = \frac{1}{2}\,\Gamma_{\Sigma^0\to\gamma\Lambda}\,\mathrm{Br}_{\Lambda\to\pi^- p}\,(1 - \alpha_\Lambda \alpha_{\Sigma^0}\cos\theta) \tag{4.6}$$

where θ is the angle between the proton and the photon in the Λ rest frame. To reconnect to the discussion at the beginning of this chapter, it is instructive to point out that Eq. (4.6) can be related to Eq. (4.1) by identifying $\boldsymbol{P} = -\alpha_{\Sigma^0}\,\hat{\boldsymbol{n}}_\gamma$. In this interpretation, the first decay process, $\Sigma^0 \to \Lambda\gamma$, is responsible for the non-zero polarization of the Λ, which is then detected through its weak decay. The experimental value of the decay asymmetry parameter α_{Σ^0} is still to be measured; a theoretical estimate is given in paper III. On the other hand, the parameter α_Λ is known [111].

The same strategy can be applied to the antiparticle decay, so that an observable to test CP symmetry can be constructed as

$$|\mathscr{O}_{\mathrm{CP}}| := |\alpha_{\Sigma^0} + \alpha_{\bar{\Sigma}^0}|.$$

Conservation of CP symmetry would result in $\mathscr{O}_{\mathrm{CP}} = 0$. An upper limit of 6.0×10^{-14} is obtained in paper III for this specific case. Obviously, no experimental facility is sensitive to this extremely tiny number. Sensational, yet unexpected, would be to observe a larger value since that would imply physics beyond the SM.

5. Summary in Swedish

Men hjärtat i en sann student
kan ingen tid förfrysa,
den glädjeeld som där han tänt,
hans hela liv skall lysa.

Eugen Höfling

Teet jag dricker, stolen jag sitter på, handen som skriver denna mening; dessa är uppenbarligen olika objekt ur min synvinkel. Jag kan skilja på dem genom att titta på dem. Däremot finns det objekt som är så små att det inte går att se med blotta ögat. Numera har vi möjligheten att undersöka dessa objekts inre struktur utöver våra ögons upplösning, till och med bortom alla slags mikroskop. Med hjälp av partikelacceleratorer kan vi dra slutsatsen att de i grund och botten består av samma beståndsdelar. Och detta gäller all synlig materia i allmänhet. Detta betyder dock inte att alla fysikproblem behöver formuleras och lösas genom att beskriva de mest elementära byggstenarna. Beroende på de frågor man vill besvara bör rätt detaljnivå väljas för att hantera fysiken i en viss skala. I själva verket kan både fysiken och dess relevanta *frihetsgrader* se mycket annorlunda ut beroende på skalan som beaktas.

Den här avhandlingen undersöker egenskaperna hos materia i extremt liten skala, den så kallade *femtometerskalan*, som ungefär motsvarar protonens storlek. En femtometer är 10^{-15} meter. Den synliga materien i universum består av atomer, som i sin tur är uppbyggda av elektroner och *nukleoner*, d.v.s. neutroner och protoner. Tittar man ännu djupare så visar det sig att även nukleonerna är sammansatta föremål, uppbyggda av elementära partiklar som kallas *kvarkar*. Det finns sex olika typer av kvarkar, kallade *smaker*. Dessa smaker är, i stigande massa: upp (u), ner (d), sär (s), charm (c), botten (b) och topp (t). Utöver kvarkar finns den andra familjen av materiapartiklar, nämligen *leptoner*. Totalt så finns det sex stycken leptoner. Dessa är: elektronen (e), myonen (μ) och tau-leptonen (τ) samt deras motsvarande neutrino $(\nu_e, \nu_\mu, \nu_\tau)$. För varje partikel finns också en motsvarande *antipartikel*. En antipartikel har samma massa som sin motsvariga partikel, men dess laddningar som t.ex. elektrisk laddning har omvänt tecken. Kvarkar (och antikvarkar) kan slås samman och bilda *hadroner*. Eftersom varje hadron har enskilda egenskaper som beror på de grundläggande beståndsdelarna så används kvarkarnas smaker som frihetsgrader för att skilja mellan hadroner. Det finns två huvudsakliga klasser

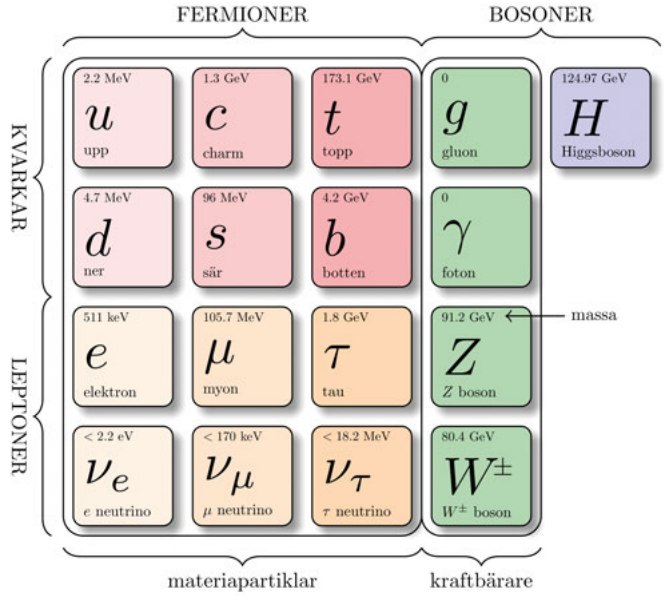

Figure 5.1. De elementära partiklarna i standardmodellen.

av hadroner: *mesoner* och *baryoner*. En meson består av en kvark och en antikvark, medan baryoner (antibaryoner) består av tre kvarkar (antikvarkar). Vi är gjorda av baryonisk materia såväl som allt runt omkring oss. Till exempel innehåller protonen två uppkvarkar och en nedkvark, vice versa för neutronen. Detta är dock en mycket förenklad bild. Kvarkarna inuti en hadron hålls samman av andra partiklar, kallade *gluoner*, som förmedlar den starka kraften. I naturen finns fyra fundamentala krafter: den starka, den elektromagnetiska, den svaga och gravitationen. Inom partikelfysiken så beskrivs dessa krafter med partiklar som kallas *bosoner*. Den mer bekanta fotonen förmedlar den elektromagnetiska kraften. De massiva bosonerna Z och $W^{\pm}$ förmedlar den svaga kraften. Hittills har gravitationens kraftbärare, *gravitonen*, inte hittats. Vidare, vid de energier som är relevanta för denna avhandling, är gravitationen mycket svagare än de andra krafterna och beaktas därför inte. I figur 5.1 samlas och grupperas alla dessa elementära partiklar i olika kategorier beroende på deras art. *Standardmodellen*, som är den grundläggande teorin för de elementära partiklarna, bygger på dessa ingredienser och beskriver deras interaktioner. Sist men inte minst har vi *Higgsbosonen*, som är en biprodukt av en teoretisk mekanism som ger massor till materiapartiklarna och kraftbärarna i en teoretisk ram som inte tillåter detta till att börja med. Detta kallas *spontan symmetribrott*, eller mer specifikt *Higgsmekanismen*.

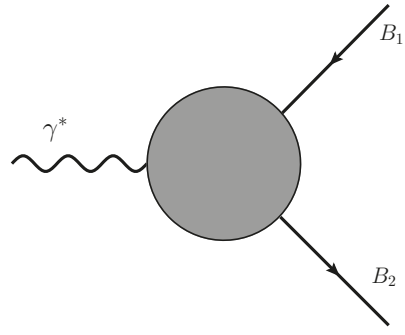

Figure 5.2. Ett diagram med en foton γ^* kopplar ihop till en inkommande baryon B_1 och utgående baryon B_2. Den gråa cirkeln representerar formfaktorer. Om baryonerna B_1 och B_2 är olika så representerar den gråa cirkeln övergångsformfaktorer.

När man bygger en teori så använder man ofta *symmetrier*. En teori sägs ha en symmetri om den är oförändrad, eller *invariant*, under en transformation som definierar symmetrin. Symmetrier är viktiga då de begränsar teorins beteende. Till exempel så finns Poincarésymmetrin som tvingar alla partiklar att bevara energi och rörelsemängd. I synnerhet har standardmodellen en *gaugesymmetri*. "Gauge" betyder att motsvarande transformationer inte är globala utan istället beror på rymdtid. Och det är denna symmetri som introducerar kraftbärarna i teorin.

Standardmodellen är inte direkt tillämplig vid energiskalan som är relevant för min avhandling. Istället är hadronerna de relevanta frihetsgraderna. Därför använder jag en *effektiv fältteori* som har baryoner och mesoner som frihetsgrader, istället för de mest grundläggande kvarkarna och gluonerna. Denna teori heter *Chiral Perturbation Theory*. Hur som helst, den bygger på samma symmetrier som karaktäriserar den starka kraften inom standardmodellen.

Det är intressant att studera hur egenskaperna hos materia med särtal skiljer sig från vanlig materia uppbyggt av nukleoner; vad händer om en av upp eller nerkvarkarna i en nukleon ersätts av en särkvark? Dessa hadroner med särkvarkar kallas *hyperoner* och kan betraktas som nukleonens syskon. Hyperoner spelar en dominerande roll i denna avhandling.

För att beskriva den inre strukturen hos hadroner har kärnfysiker infört funktioner som kallas *formfaktorer*. Dessa funktioner kvantifierar skillnaden mellan en punktformig partikel och en partikel med en inre struktur. Den elektromagnetiska interaktionen, d.v.s. fotonerna, fungerar som ett diagnostiskt verktyg för att utforska de rumsliga fördelningarna av elektrisk laddning och magnetiseringstäthet inuti hadronerna. Av denna anledning så ges formfaktorer som funktioner av fotonimpuls i kvadrat q^2. Formfaktorerna kan mätas experimentellt och kan förutsägas av teoretiker. I diagrammet i figur 5.2 representeras de elektromagnetiska formfaktorerna av en grå cirkel istället för ett punkt eftersom de undersöker den sammansatta objekten i sig. Ett fo-

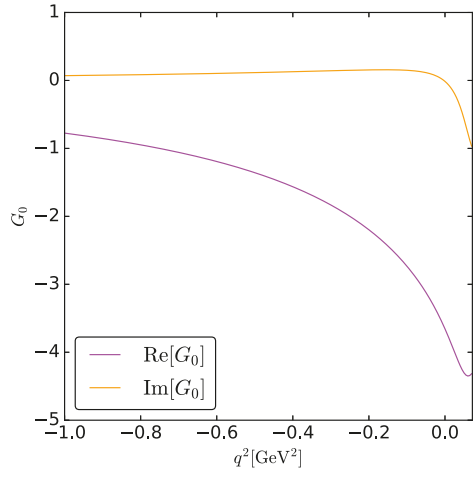

Figure 5.3. De reella och imaginära delarna av $G_0(q^2)$, en av de tre elektromagnetiska formfaktorer hos Σ^*-Λ hyperonövergången.

ton, betecknat γ^*, kopplar ihop till en inkommande baryon B_1 och till en utgående baryon B_2. I fallet där B_1 och B_2 är samma typ av baryon så motsvarar den gråa cirkeln baryonens formfaktorer. I det andra fallet där B_1 och B_2 är olika talar man om *övergångsformfaktorer*. Omfattande studier har utförts för nukleonernas formfaktorer. Men när det kommer till hyperoner är den nuvarande kunskapen om (övergångs) formfaktorer är mycket begränsad. Tack vare matematiska verktyg som *dispersionsförhållanden* har jag kunnat göra förutsägelser för övergångsformfaktorer för Σ-Λ och Σ^*-Λ hyperoner, vid låga energier. Ett dispersionsförhållande består av en integral som relaterar den verkliga och den imaginära delen av en analytisk funktion till varandra. Detta är mycket kraftfullt matematiskt verktyg; det räcker med att känna till den imaginära delen av en funktion i en viss region av fotonimpulsen q^2 för att kunna göra förutsägelser av funktionen för alla q^2-värden. När det kommer till hyperoner är det svårt att experimentellt mäta den negativa q^2-regionen. Detta beror på det faktum att hyperoner är instabila partiklar och därför sönderfaller de efter en relativt kort tid. I figur 5.3 visas teoretiska förutsägelser för en av de tre Σ^*-Λ övergångsformfaktorer som sträcker sig över den låga, negativa q^2-regionen. Detta är ett första steg mot en komplett förståelse av hur den elektriska laddningen fördelas inuti dessa hyperoner. Det framtida experimentet PANDA som byggs utanför Darmstadt, Tyskland, kommer att utföra nya mätningar av hyperoner. Dessa mätningar kommer ge teoretikerna för närvarande saknad information, som behövs för att förbättra noggrannheten i förutsägelserna. Det långsiktiga målet är att jämföra hyperonernas och nukleonernas formfaktorer för att få en djupare insikt i beteendet hos kvarkarna inuti dessa hadroner.

Hyperonerna visar sig också vara ett utmärkt verktyg i andra frågeställningar. En del av mitt arbete handlar om frågan om asymmetrin av materia och antimateria i universum. Mängden materia i vårt universum observeras vara mycket större än antimateria. Detta är ett faktum då vi inte skulle existera om mängderna var lika. Än så länge har vi ingen förklaring till denna asymmetri. Ett av det nödvändiga villkoret för att detta ska ske är en brytning av den så kallade *CP-symmetrin*. Denna symmetri innebär att ett system måste vara invariant när alla laddningar samt de tre rumsliga dimensionerna byter tecken. Standardmodellen förutsäger inte tillräckligt med CP-brott. Därför letar experimentalister insisterande efter nya möjliga källor till CP-brott, och teoretiker undersöker utvidgningar av standardmodellen som skulle möjliggöra mer brytning av CP-symmetrin. Min forskning tar också upp denna fråga. I synnerhet har jag bidragit till att utveckla en kraftfull formalism som gör det möjligt att systematiskt leta efter CP-brott. Samtidigt kan denna formalism användas för att härleda fördelningar hos sönderfallsprodukterna från hyperonsönderfall. Med hjälp av dessa fördelningar kan *polarisationen* hos hyperonerna mätas. Polarisationen är en observabel som kvantifierar hyperonernas spinnriktning och kan uppstå som en konsekvens av produktionsmekanismen som skapade hyperonerna. Genom att studera polarisationen kan vi därför studera produktionsprocessen som kan förmedlas av den starka eller elektromagnetiska kraften och förbättra vår förståelse av produktionsmekanismen.

Acknowledgements

As happens sometimes, a moment settled and hovered and remained for much more than a moment. And sound stopped and movement stopped for much, much more than a moment.

John Steinbeck, Of Mice and Men

During my PhD, I have realized that getting stuck on a problem is a necessary step to make progress. It sounds trivial, but it definitely took some time before I could accept it. With this new attitude, I see now challenges as part of the learning process: one needs some immersion time before getting a good idea, no need to worry if it does not come in a day. The longer the time it takes, the greater the satisfaction afterwards.

My supervisor Stefan Leupold deserves a huge thanks. Stefan, you have been an excellent guide during these years, always enthusiastic and on-point. Thanks for sharing your knowledge on hadron physics and for being available anytime I needed your help. You and Sabrina are, in your simplicity, such extraordinary people to look up to. I also want to thank my co-supervisors Karin Schönning and Tord Johansson. In particular Karin, for introducing me to the interesting topic of hyperon physics in the very beginning and for standing out as a passionate, determined and successful woman in physics. And Tord, for believing in my PhD since before it could start. To me, you will always be the boss of the nuclear physics division. Among the senior colleagues I also had the pleasure to collaborate with Andrzej Kupść, who has an incredible intuition for particle physic. It has been very stimulating to try to translate your ideas into formulae, to then figure out that, a part from plus and minus signs, you were indeed right.

I often happen to think how lucky I have been to work at Ångström, in such a nice and stimulating environment. I will miss my office and I will definitely miss the colleagues in the divisions of nuclear and high-energy physics. You all, with quite distinct personal features, have taught me a lot during physics meeting but especially during our epic lunch discussions on all kinds of improbable things.

I am grateful for the amazing friends I have around the world. My dear high-school friends Martina, Vale and Yari live in Italy but I feel so close to them. Thanks for visiting me in Sweden multiple times and for being the most generous, critical and complex people I know. I want to thank my inseparable childhood companion Lucilla for bringing back funny memories every time

we meet. I am also glad to keep in regular contact with my old friends from the bachelor studies in Turin. In particular Umbi, which is a special person to me. Thank you because, despite being scattered all over the world, we support and care about each other. On the other hand, when in need of some comprehension here in Sweden, Sara and Andrea have always been present. When in abstinence of a good pizza, they always have a solution. This I value as true friendship!

A big thanks goes to the *dansförening* Swingkatten, where I have been active since the first day I moved to Sweden. The happy moments I had training, teaching and social dancing through the years are uncountable. I believe I have met long-life friends through the dance. In particular I want to thank Per, Benjaminas and Petros for having significantly contributed to my passion for swing dancing. Veronika and Nils, Erik and Lina for teaching me Swedish while dancing and for the delicious dinners together. Thanks to the members of the show group *MessAround*; I am so incredibly proud of being able to perform with you all!

The last acknowledgments are addressed to my beautiful family, starting from my grandparents, who surely contributed greatly to shape my character since an early age. I want to thank zio Gulberto for being a grownup with the curiosity of a child. This makes you the best possible uncle I could have ever wished for. I want to thank my sister Giulia, for being able to bring order in my chaotic life with a simple phone call. I do not know how you do it, but it has happened several times, magically. I have been thinking for quite some time why exactly I want to thank my parents; I have a long list but there is one thing in particular I am grateful for. Thanks for giving me the possibility to continue the studies abroad. And when I say possibility, I do not mean permission or economical support, I mean it in a broader sense. Since I was a kid, you have been teaching me to not fear cultural diversity. Outside my little hometown Castellamonte, it is neither better, nor worse. It is just different. Therefore, I have always enjoyed exploring and adapting to foreign habits, instead of being scared of leaving the nest. Thanks to this strength, I had the possibility to move abroad and expand my horizons beyond what I could have imagined. Finally, I want to thank Walter for sharing the simple things of everyday life with me; if done with care they become the most precious.

References

[1] C. L. Bennett et al. Nine-year Wilkinson Microwave Anisotropy Probe (WMAP) observations: Final maps and results. *Astrophys. J. Supp.*, 208:20, 2013.

[2] M. Gell-Mann. The Eightfold Way: A theory of strong interaction symmetry. Report No. CTSL-20, 1961.

[3] Y. Ne'eman. Derivation of strong interactions from a gauge invariance. *Nucl. Phys.*, 26:222, 1961.

[4] M. Gell-Mann. Symmetries of baryons and mesons. *Phys. Rev.*, 125:1067, 1962.

[5] V.E. Barnes et al. Observation of a Hyperon with Strangeness Minus Three. *Phys. Rev. Lett.*, 12:204, 1964.

[6] M. Gell-Mann. A Schematic Model of Baryons and Mesons. *Phys. Lett.*, 8:214, 1964.

[7] G. Zweig. An SU(3) model for strong interaction symmetry and its breaking. Report No. CERN-TH-401, 1964.

[8] H. Fritzsch, Murray Gell-Mann, and H. Leutwyler. Advantages of the Color Octet Gluon Picture. *Phys. Lett. B*, 47:365, 1973.

[9] O.W. Greenberg. Spin and Unitary Spin Independence in a Paraquark Model of Baryons and Mesons. *Phys. Rev. Lett.*, 13:598, 1964.

[10] M. Breidenbach et al. Observed behavior of highly inelastic electron-proton scattering. *Phys. Rev. Lett.*, 23:935, 1969.

[11] R. Frisch and O. Stern. Über die magnetische Ablenkung von Wasserstoffmolekülen und das magnetische Moment des Protons. *Zeitschrift fur Physik*, 85:4, January 1933.

[12] M. E. Peskin and D. V. Schroeder. *An introduction to quantum field theory*. Addison-Wesley, 1995.

[13] M. Srednicki. *Quantum field theory*. Cambridge University Press, 2007.

[14] M. D. Schwartz. *Quantum Field Theory and the Standard Model*. Cambridge University Press, 2014.

[15] J.F. Donoghue, E. Golowich, and B. R. Holstein. *Dynamics of the standard model*. Cambridge University Press, 1992.

[16] C. Itzykson and J. B. Zuber. *Quantum Field Theory*. International Series in Pure and Applied Physics. McGraw-Hill, 1980.

[17] F. Englert and R. Brout. Broken Symmetry and the Mass of Gauge Vector Mesons. *Phys. Rev. Lett.*, 13:321, 1964.

[18] P. W. Higgs. Broken Symmetries and the Masses of Gauge Bosons. *Phys. Rev. Lett.*, 13:508, 1964.

[19] Y. Fukuda et al. Evidence for oscillation of atmospheric neutrinos. *Phys. Rev. Lett.*, 81:1562, 1998.

[20] Q. R. Ahmad et al. Direct evidence for neutrino flavor transformation from neutral current interactions in the Sudbury Neutrino Observatory. *Phys. Rev. Lett.*, 89:011301, 2002.
[21] T. Araki et al. Measurement of neutrino oscillation with KamLAND: Evidence of spectral distortion. *Phys. Rev. Lett.*, 94:081801, 2005.
[22] J. Goldstone. Field Theories with Superconductor Solutions. *Nuovo Cim.*, 19:154, 1961.
[23] G.C. Branco et al. Theory and phenomenology of two-Higgs-doublet models. *Phys. Rept.*, 516:1, 2012.
[24] R. Alkofer and J. Greensite. Quark Confinement: The Hard Problem of Hadron Physics. *J. Phys.*, G34:S3, 2007.
[25] C. Gattringer and C. B. Lang. Quantum chromodynamics on the lattice. *Lect. Notes Phys.*, 788:1, 2010.
[26] D. J. Gross and F. Wilczek. Ultraviolet Behavior of Nonabelian Gauge Theories. *Phys. Rev. Lett.*, 30:1343, 1973.
[27] H. D. Politzer. Reliable Perturbative Results for Strong Interactions? *Phys. Rev. Lett.*, 30:1346, 1973.
[28] S. Weinberg. *The quantum theory of fields. Vol. 2: Modern applications*. Cambridge University Press, 2005.
[29] R. D. Peccei. The Strong CP problem and axions. *Lect. Notes Phys.*, 741:3, 2008.
[30] C.A. Baker et al. An improved experimental limit on the electric dipole moment of the neutron. *Phys. Rev. Lett.*, 97:131801, 2006.
[31] J. J. Sakurai. *Invariance Principles and Elementary Particles*. Princeton University Press, 1964.
[32] A. D. Sakharov. Violation of CP invariance, C asymmetry, and baryon asymmetry of the universe. *JETP Lett.*, 5:24, 1967.
[33] W. Bernreuther. CP violation and baryogenesis. *Lect. Notes Phys.*, 591:237, 2002.
[34] J.H. Christenson, J.W. Cronin, V.L. Fitch, and R. Turlay. Evidence for the 2π Decay of the K_2^0 Meson. *Phys. Rev. Lett.*, 13:138, 1964.
[35] J. S. Schwinger. The theory of quantized fields. 1. *Phys. Rev.*, 82:914, 1951.
[36] G. Luders. On the Equivalence of Invariance under Time Reversal and under Particle-Antiparticle Conjugation for Relativistic Field Theories. *Kong. Dan. Vid. Sel. Mat. Fys. Med.*, 28N5:1, 1954.
[37] M. Kobayashi and T. Maskawa. CP Violation in the Renormalizable Theory of Weak Interaction. *Prog. Theor. Phys.*, 49:652, 1973.
[38] G. Steigman. Observational tests of antimatter cosmologies. *Ann. Rev. Astron. Astrophys.*, 14:339, 1976.
[39] B. Kubis and U. G. Meißner. Baryon form-factors in chiral perturbation theory. *Eur. Phys. J.*, C18:747, 2001.
[40] J. M. Alarcón, A. N. Hiller Blin, M. J. Vicente Vacas, and C. Weiss. Peripheral transverse densities of the baryon octet from chiral effective field theory and dispersion analysis. *Nucl. Phys.*, A964:18, 2017.
[41] BESIII Collaboration. Complete Measurement of the Λ Electromagnetic Form Factors. *Phys. Rev. Lett.*, 123:122003, 2019.
[42] HADES Collaboration. Σ^0 production in proton nucleus collisions near

threshold. *Phys. Lett.*, B781:735, 2018.
[43] HADES Collaboration. Time-Like Baryon Transitions in Hadroproduction. *Few Body Syst.*, 59:141, 2018.
[44] HADES Collaboration. Proposals for experiments at SIS18 during FAIR Phase-0. Report No. GSI-2019-00976, 2017.
[45] PANDA Collaboration. Physics Performance Report for PANDA: Strong Interaction Studies with Antiprotons. 2009. arXiv: 0903.3905.
[46] K. Schönning. Strong Interaction Studies with PANDA at FAIR. *EPJ Web Conf.*, 125:01006, 2016.
[47] E. Thomé. *Multi-Strange and Charmed Antihyperon-Hyperon Physics for PANDA*. PhD thesis, Uppsala University, 2012.
[48] H. Georgi. Effective field theory. *Ann. Rev. Nucl. Part. Sci.*, 43:209, 1993.
[49] A. V. Manohar. Effective field theories. *Lect. Notes Phys.*, 479:311, 1997.
[50] C.P. Burgess. Introduction to Effective Field Theory. *Ann. Rev. Nucl. Part. Sci.*, 57:329, 2007.
[51] J. Gasser and H. Leutwyler. Chiral Perturbation Theory to One Loop. *Annals Phys.*, 158:142, 1984.
[52] J. Gasser and H. Leutwyler. Chiral Perturbation Theory: Expansions in the Mass of the Strange Quark. *Nucl. Phys.*, B250:465, 1985.
[53] S. Weinberg. Phenomenological Lagrangians. *Physica*, A96:327, 1979.
[54] U. G. Meißner. Recent developments in chiral perturbation theory. *Rept. Prog. Phys.*, 56:903, 1993.
[55] A. Pich. Chiral perturbation theory. *Rept. Prog. Phys.*, 58:563, 1995.
[56] G. Ecker. Chiral perturbation theory. *Prog. Part. Nucl. Phys.*, 35:1, 1995.
[57] V. Bernard and U. G. Meißner. Chiral perturbation theory. *Ann. Rev. Nucl. Part. Sci.*, 57:33, 2007.
[58] J. Bijnens. Chiral perturbation theory beyond one loop. *Prog. Part. Nucl. Phys.*, 58:521, 2007.
[59] S. Scherer. Introduction to chiral perturbation theory. *Adv. Nucl. Phys.*, 27:277, 2003.
[60] S. Scherer and M. R. Schindler. A Primer for Chiral Perturbation Theory. *Lect. Notes Phys.*, 830:1, 2012.
[61] J. Goldstone, A. Salam, and S. Weinberg. Broken Symmetries. *Phys. Rev.*, 127:965, 1962.
[62] Y. Nambu. Quasiparticles and Gauge Invariance in the Theory of Superconductivity. *Phys. Rev.*, 117:648, 1960.
[63] E. Noether. Invariant Variation Problems. *Gott. Nachr.*, 1918:235, 1918.
[64] G. 't Hooft. A Planar Diagram Theory for Strong Interactions. *Nucl. Phys.*, B72:461, 1974.
[65] R. Kaiser and H. Leutwyler. Large N_c in chiral perturbation theory. *Eur. Phys. J.*, C17:623, 2000.
[66] E. Witten. Global Aspects of Current Algebra. *Nucl. Phys.*, B223:422, 1983.
[67] J. Wess and B. Zumino. Consequences of anomalous Ward identities. *Phys. Lett.*, 37B:95, 1971.
[68] C. Terschlüsen and S. Leupold. Renormalization of the low-energy constants of chiral perturbation theory from loops with dynamical vector mesons. *Phys. Rev.*, D94:014021, 2016.

[69] J. Gasser, M. E. Sainio, and A. Švarc. Nucleons with Chiral Loops. *Nucl. Phys.*, B307:779, 1988.
[70] N. Fettes, U.G. Meißner, M. Mojžiš, and S. Steininger. The chiral effective pion nucleon Lagrangian of order p**4. *Annals Phys.*, 283:273, 2000. [Erratum: *Annals Phys.*, 288:249, 2001].
[71] H. Georgi. An Effective Field Theory for Heavy Quarks at Low-energies. *Phys. Lett.*, B240:447, 1990.
[72] V. Bernard, N. Kaiser, J. Kambor, and U. G. Meißner. Chiral structure of the nucleon. *Nucl. Phys.*, B388:315, 1992.
[73] E. E. Jenkins and A. V. Manohar. Baryon chiral perturbation theory using a heavy fermion Lagrangian. *Phys. Lett.*, B255:558, 1991.
[74] M. E. Luke and A. V. Manohar. Reparametrization invariance constraints on heavy particle effective field theories. *Phys. Lett.*, B286:348, 1992.
[75] J. Gegelia and G. Japaridze. Matching heavy particle approach to relativistic theory. *Phys. Rev. D*, 60:114038, 1999.
[76] T. Fuchs, J. Gegelia, G. Japaridze, and S. Scherer. Renormalization of relativistic baryon chiral perturbation theory and power counting. *Phys. Rev.*, D68:056005, 2003.
[77] T. Becher and H. Leutwyler. Baryon chiral perturbation theory in manifestly Lorentz invariant form. *Eur. Phys. J.*, C9:643, 1999.
[78] T. R. Hemmert, B. R. Holstein, and J. Kambor. Heavy baryon chiral perturbation theory with light deltas. *J. Phys.*, G24:1831, 1998.
[79] V. Pascalutsa and D. R. Phillips. Effective theory of the $\Delta(1232)$ in Compton scattering off the nucleon. *Phys. Rev.*, C67:055202, 2003.
[80] W. Rarita and J. Schwinger. On a theory of particles with half integral spin. *Phys. Rev.*, 60:61, 1941.
[81] E. E. Jenkins and A. V. Manohar. Chiral corrections to the baryon axial currents. *Phys.Lett.*, B259:353, 1991.
[82] V. Pascalutsa, M. Vanderhaeghen, and S. N. Yang. Electromagnetic excitation of the $\Delta(1232)$-resonance. *Phys. Rept.*, 437:125, 2007.
[83] T. Ledwig, J. Martin Camalich, L. S. Geng, and M. J. Vicente Vacas. Octet-baryon axial-vector charges and SU(3)-breaking effects in the semileptonic hyperon decays. *Phys. Rev.*, D90:054502, 2014.
[84] J. J. Sakurai. *Currents and Mesons*. University of Chicago Press, 1969.
[85] C. Terschlüsen. *Theoretical Studies of Hadronic Reactions with Vector Mesons*. PhD thesis, Uppsala University, 2016.
[86] J. F. Donoghue, J. Gasser, and H. Leutwyler. The Decay of a Light Higgs Boson. *Nucl. Phys. B*, 343:341, 1990.
[87] John F. Donoghue. Dispersion relations and effective field theory. In *Advanced School on Effective Theories*, 1996. arXiv: hep-ph/9607351.
[88] G. Colangelo, J. Gasser, and H. Leutwyler. $\pi\pi$ scattering. *Nucl. Phys.*, B603:125, 2001.
[89] R. Garcia-Martin et al. The pion-pion scattering amplitude. IV: Improved analysis with once subtracted Roy-like equations up to 1100 MeV. *Phys. Rev.*, D83:074004, 2011.
[90] R.E. Cutkosky. Singularities and discontinuities of Feynman amplitudes. *J. Math. Phys.*, 1:429, 1960.

[91] S. Leupold. The nucleon as a test case to calculate vector-isovector form factors at low energies. *Eur. Phys. J. A*, 54:1, 2018.
[92] R. Karplus, C. M. Sommerfield, and E. H. Wichmann. Spectral Representations in Perturbation Theory. 1. Vertex Function. *Phys. Rev.*, 111:1187, 1958.
[93] M. Tanabashi and others (PDG). Review of particle physics. *Phys. Rev. D*, 98:030001, Aug 2018.
[94] LHCb Collaboration. Measurement of matter-antimatter differences in beauty baryon decays. *Nature Phys.*, 13:391, 2017.
[95] J. J. Sakurai and J. Napolitano. *Modern quantum physics*. Cambridge University Press, 2017.
[96] M. G. Doncel, P. Mery, L. Michel, P. Minnaert, and K. C. Wali. Properties of polarization density matrix in Regge pole models. *Phys. Rev. D*, 7:815, 1973.
[97] M. G. Doncel, L. Michel, and P. Minnaert. Rigorous spin tests from usual strong decays. *Nucl. Phys. B*, 38:477, 1972.
[98] W. Ikegami Andersson. *Exploring the Merits and Challenges of Hyperon Physics*. PhD thesis, Uppsala University, 2020.
[99] E. Klempt et al. Antinucleon nucleon interaction at low energy: Scattering and protonium. *Phys. Rept.*, 368:119, 2002.
[100] P. G. Ortega, D. R. Entem, and F. Fernandez. $p\bar{p} \to \Lambda\bar{\Lambda}$ depolarization and spin transfer in a constituent quark model. *Phys. Lett.*, B696:352, 2011.
[101] J. Haidenbauer, T. Hippchen, K. Holinde, B. Holzenkamp, V. Mull, and J. Speth. The reaction $\bar{p}p \to \bar{\Lambda}\Lambda$ in the meson exchange picture. *Phys. Rev. C*, 45:931, 1992.
[102] J. Haidenbauer, K. Holinde, V. Mull, and J. Speth. Meson exchange and quark-gluon transitions in the $\bar{p}p \to \bar{\Lambda}\Lambda$ process. *Phys. Rev. C*, 46:2158, 1992.
[103] M. Jacob and G. C. Wick. On the General Theory of Collisions for Particles with Spin. *Annals Phys.*, 7:404, 1959.
[104] A.Z. Dubnickova, S. Dubnicka, and M.P. Rekalo. Investigation of the nucleon electromagnetic structure by polarization effects in $e^+e^- \to N\bar{N}$ processes. *Nuovo Cim. A*, 109:241, 1996.
[105] H. Czyż, A. Grzelińska, and J. H. Kühn. Spin asymmetries and correlations in Λ-pair production through the radiative return method. *Phys. Rev. D*, 75:074026, 2007.
[106] E. Tomasi-Gustafsson, F. Lacroix, C. Duterte, and G. I. Gakh. Nucleon electromagnetic form-factors and polarization observables in space-like and time-like regions. *Eur. Phys. J.*, A24:419, 2005.
[107] G. Fäldt and A. Kupść. Hadronic structure functions in the $e^+e^- \to \bar{\Lambda}\Lambda$ reaction. *Phys. Lett.*, B772:16, 2017.
[108] S. Pacetti. Nucleon form factors and dispersion relations. *Eur. Phys. J.*, A32:421, 2007.
[109] J. Haidenbauer and U. G. Meißner. The electromagnetic form factors of the Λ in the timelike region. *Phys. Lett.*, B761:456, 2016.
[110] F. K. Guo and U. G. Meißner. Baryon electric dipole moments from strong CP violation. *JHEP*, 12:097, 2012.
[111] M. Ablikim et al. Polarization and entanglement in baryon-antibaryon pair production in electron-positron annihilation. *Nature Physics*, 15:631, 2019.

Acta Universitatis Upsaliensis

Digital Comprehensive Summaries of Uppsala Dissertations from the Faculty of Science and Technology 1939

Editor: The Dean of the Faculty of Science and Technology

A doctoral dissertation from the Faculty of Science and Technology, Uppsala University, is usually a summary of a number of papers. A few copies of the complete dissertation are kept at major Swedish research libraries, while the summary alone is distributed internationally through the series Digital Comprehensive Summaries of Uppsala Dissertations from the Faculty of Science and Technology. (Prior to January, 2005, the series was published under the title "Comprehensive Summaries of Uppsala Dissertations from the Faculty of Science and Technology".)

Distribution: publications.uu.se
urn:nbn:se:uu:diva-406648

ACTA
UNIVERSITATIS
UPSALIENSIS
UPPSALA
2020